Analytical Methods

ROYAL SOCIETY OF CHEMISTRY

MINIREVIEW

View Article Online
View Journal | View Issue

Cite this: *Anal. Methods*, 2016, **8**, 3419

Published on 05 April 2016. Downloaded by DTU Library on 4/3/2020 2:12:37 PM.

Low energy ion scattering (LEIS). A practical introduction to its theory, instrumentation, and applications

Cody V. Cushman,[a] Philipp Brüner,[b] Julia Zakel,[b] George H. Major,[a] Barry M. Lunt,[c] Nicholas J. Smith,[d] Thomas Grehl*[b] and Matthew R. Linford*[a]

Received 15th March 2016
Accepted 1st April 2016

DOI: 10.1039/c6ay00765a

www.rsc.org/methods

Low energy ion scattering (LEIS) probes the elemental composition of the outermost atomic layer of a material and provides static depth profiles of the outer *ca.* 10 nm of surfaces. Its extreme surface sensitivity and quantitative nature make it a powerful tool for studying the relationships between surface chemistry and surface related phenomena such as wetting, adhesion, contamination, and thin film growth. The high depth resolution obtained in LEIS in its static and sputter depth profile modes are useful for studying the layer structures of thin films. LEIS instrumentation has improved significantly in recent years, showing dramatic increases in its sensitivity and further expanding its potential applications. In this article, we provide a practical introduction to the technique, including a discussion of the basic theory of LEIS, LEIS spectra, LEIS instrumentation, and LEIS applications, including catalysts, solid oxide fuel cells (SOFCs), and thin films in integrated circuits.

1. Overview

Atoms at the surface of a material are generally in a different chemical environment than those buried within the bulk. This often results in important compositional and morphological differences between the surface of a material and its interior. For example, surface-bound water molecules experience very different environments than those in bulk water. Surface composition is important because materials interact with their surroundings through their surfaces, and many important phenomena are governed by their surfaces, including wetting, adhesion, contamination, reactivity, corrosion, and catalysis. Because understanding these phenomena is so important, the analysis of surfaces and interfaces has become an important and specialized area of analytical chemistry.

Analyzing surface composition is challenging because, in general, only a relatively small portion of a material is actually at the surface and available for analysis. Surface analysis techniques must be sensitive enough to obtain information from a very small sample volume before damage from the analysis significantly alters the surface. They must also be sufficiently discriminating to differentiate between signals originating from the surface and bulk. The challenge of obtaining information from a surface often increases as the depth of analysis decreases—fewer atoms/molecules become available for analysis, and contamination or damage during the analysis become increasingly important considerations. Depths of analysis in surface studies range from a single atomic layer to a few hundred nm.

In this work, we provide a practical introduction to low energy ion scattering (LEIS). LEIS is an extremely versatile surface analysis technique that is performed under ultra-high vacuum (UHV) conditions. LEIS is specifically sensitive to the elemental composition of the *outermost* atomic layer of a material, and additionally provides depth profile information about its outer *ca.* 10 nm. Information from deeper within the material can be obtained *via* LEIS sputter depth profiling. Sensitivity to the elemental composition of the outer atomic layer of a material is LEIS's principle asset. Indeed, it is the only technique of which we are aware with its degree of surface sensitivity and specificity. Therefore, LEIS is a powerful tool for understanding the relationship between surface composition and material properties. Here we provide an overview of the basic theory of LEIS, LEIS instrumentation, quantitation in LEIS, LEIS depth profiling, and applications of the technique to catalysts, semiconductor materials, and solid-oxide fuel cells (SOFCs). In particular, we discuss how recent advances in LEIS instrumentation have dramatically improved the limit of detection of the method. This article is not intended to be a comprehensive review on the topic, but rather a practical introduction. A more detailed description of the theory and development of the technique can be found elsewhere,[1–5] particularly in a review by Brongersma and coworkers.[6]

[a]Chemistry and Biochemistry, Brigham Young University, Provo, UT 84602, USA. E-mail: mrlinford@chem.byu.edu
[b]ION-TOF GmbH, Heisenbergstr. 15, 48149 Muenster, Germany. E-mail: thomas.grehl@iontof.com
[c]Information Technology, Brigham Young University, Provo, UT 84602, USA
[d]Science and Technology Division, Corning Incorporated, Corning, NY 14831, USA

Published on 05 April 2016. Downloaded by DTU Library on 4/3/2020 2:12:37 PM.

2. Introduction to the theory of LEIS[7]

LEIS has existed as a technique since the late 1960's, but recent advances in instrumentation have dramatically improved its capabilities and applicability.[1,2,6,8] Unlike X-ray photoelectron spectroscopy (XPS) and time-of-flight secondary ion mass spectrometry (ToF-SIMS), which sample the first few nanometers of materials, LEIS is sensitive to their outermost atomic layer.[1,2,6,8,9] That is, XPS and ToF-SIMS give incredibly useful information about the outer few nanometers of materials, where to some degree they average this information, but they struggle to provide definitive information about the final atomic layer of a material.[10] Thus, LEIS occupies an important niche that will likely become more important with time, where, again, LEIS is a powerful tool for understanding the relationship between surface composition and important phenomena such as catalysis, wetting, diffusion, adhesion, and adsorption.[6,11–14] In this section, we discuss the basic theory of LEIS, which will include an introduction to interpreting LEIS spectra.

Surface instrumentation is often categorized based on the probing species that is directed onto a surface and what leaves it. In XPS, X-rays enter the surface and photoelectrons (energetic electrons) exit. In ToF-SIMS, primary ions bombard the surface and secondary ions are emitted. Scanning electron microscopy has electrons in and electrons out. LEIS probes a surface with noble gas ions, and then detects the same backscattered ions (see Fig. 1). There is an obvious similarity between LEIS and Rutherford backscattering (RBS), which is also based on the backscattering of atoms.[2,15] The primary difference between RBS and LEIS is the energy of the incoming ions. LEIS uses a *ca.* 1 to 10 keV beam of noble gas ions, while RBS uses primary ions with MeV energies. For this reason, RBS is essentially a bulk technique, probing on the order of a micron into materials. The much lower energy primary ions in LEIS are significantly less penetrating. Furthermore, the noble gas ions that are used in LEIS have a high probability of being neutralized when they interact with a material. Since only ions are detected in LEIS, and only ions that scatter off of the outermost atomic layer of a material have short enough interaction times to avoid neutralization, LEIS is uniquely sensitive to the atomic composition of the outermost layer of a material.[2,9,16] Indeed, LEIS is so surface sensitive that even a monolayer of contamination, *e.g.*, adventitious carbon, can obscure the signal from a material.

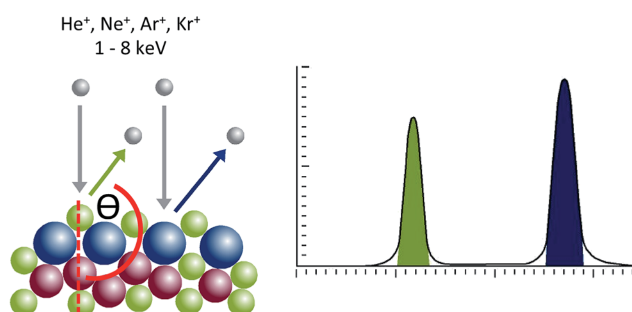

Fig. 1 (Left) Noble gas ion bombardment of a surface with two types of exposed atoms. (Right) LEIS signal corresponding to the surface on the left. Note that there is no LEIS signal from the 'red' atoms.

Eqn (1) is the governing equation of LEIS. A list of its underlying assumptions can be found in an article by Smith.[1]

$$E_S = kE_P = \left(\frac{\cos\Theta + \sqrt{\left(\frac{M_S}{M_P}\right)^2 - \sin^2\Theta}}{1 + \frac{M_S}{M_P}} \right)^2 E_P, \quad \frac{M_S}{M_P} \geq 1 \quad (1)$$

The variables in this equation are the energy of the primary ion, E_P, the energy it has after scattering, E_S, the mass of the primary ion, M_P, and the mass of the particle it scatters off of, M_S. The other variable in this equation, Θ, is the angle through which the scattering takes place (see Fig. 1). A condition for eqn (1) is that $M_S/M_P \geq 1$ (the surface atom from which scattering occurs must be heavier than the ion striking it). If this condition is not fulfilled ($M_S/M_P < 1$), *e.g.*, He^+ striking a hydrogen atom, no backscattering takes place, only forward scattering. As an analogy, imagine what would happen if the pins in a bowling alley were heavier than the bowling ball. In this case, the bowling ball would recoil upon striking a pin. This would entirely change the game. Bowling, as it stands, is based on forward scattering of the ball, not backscattering. Not to belabor the point, consider what would happen if you used a ping pong ball for bowling, which is obviously much lighter than a bowling pin. Clearly if the much lighter ping pong ball were to strike the bowling pin head on, it would bounce back in the direction from which it came. This analogy helps us appreciate how scattering depends on the masses of the projectile and the object it strikes. Because in a LEIS experiment E_P, M_P, Θ, and E_S are known or defined by the instrument, M_S can be determined. Eqn (1) can be derived entirely from classical physics using the principles of conservation of energy and momentum; the ideal scattering energy in LEIS can be described without quantum mechanics. In practice, however, there are inelastic contributions to the scattering process, which shift the measured scattering energies to slightly lower energies than those calculated using eqn (1) and give the peaks in LEIS spectra a Gaussian shape.[6]

When one encounters a new equation in physics, it is often a good idea to evaluate it in its limits. Consider the case where M_S is increasingly large compared to M_P, *e.g.*, the case of He^+ scattering off of a very heavy atom. First, we multiply eqn (1) by $(M_P/M_S)/(M_P/M_S)$, which yields

$$E_S = \left(\frac{\frac{M_P}{M_S}\cos\Theta + \frac{M_P}{M_S}\sqrt{\left(\frac{M_S}{M_P}\right)^2 - \sin^2\Theta}}{\frac{M_P}{M_S} + 1} \right)^2 E_P. \quad (2)$$

This journal is © The Royal Society of Chemistry 2016

View Article Online

Rearranging the equation, we obtain

$$E_S = \left(\frac{\frac{M_P}{M_S}\cos\Theta + \sqrt{1 - \left(\frac{M_P}{M_S}\right)^2 \sin^2\Theta}}{\frac{M_P}{M_S} + 1} \right)^2 E_P. \quad (3)$$

Now, consider the limit of $M_P/M_S \to 0$. Of course this is not physically possible, but it becomes a more reasonable approximation as M_S gets large compared to M_P, *e.g.*, $^4He^+$ scattering off of ^{238}U, which gives $M_P/M_S \approx 4/238 \approx 0.02$. In any case, as $M_P/M_S \to 0$ in eqn (3) becomes

$$E_S = E_P. \quad (4)$$

Thus, for the case of an infinitely heavy M_S atom, the energy of the scattered ion, E_S, is equal to the energy of the primary ion, E_P, *i.e.*, all the energy of the primary ion is in the backscattered ion. Fig. 2 is a plot of the percentage of the energy backscattered in LEIS as a function of M_S. The previous discussion about eqn (1) in its limit helps us understand why the curve in Fig. 2 for He^+ (the projectile) asymptotically approaches 100% at high M_S. Obviously the other curves in Fig. 2 are also approaching this limit.

LEIS identifies elements by their masses, and successful identification of an element depends upon optimizing the analysis parameters so that one nuclear mass can be distinguished from another.[6,8] The most important parameters that the user can control in LEIS are the type and energy of the ions used to probe the surface. The steepness of the curve for He^+ in Fig. 1 at lower M_S suggests that LEIS with He^+ is very discriminating to the lighter elements. For example, using eqn (1), we calculate an energy difference of 94 eV for 3 keV He^+ backscattered at 145° from ^{12}C and ^{13}C. Since the widths of these peaks will be around 80 eV, these signals can be resolved.

In contrast to the steep rise in backscattering energy at low values of M_S, the increasing flatness/asymptotic behavior of the curve in Fig. 1 for He^+ at higher M_S shows that LEIS lacks discrimination/resolution for the heavier elements with this lighter probe. For example, for 3 keV He^+ at 145° backscattering, the energy difference between ^{58}Ni and ^{59}Co is only 10 eV. LEIS also shows little discrimination between ^{208}Pb and ^{197}Au under these analysis conditions. That is, even though they have a greater mass difference, the higher masses of Pb and Au lead to an energy difference of only 11 eV between their peaks. Thus, LEIS with He^+ nicely resolves the lighter elements while it is less effective at resolving the heavier ones.

A solution to the lack of resolving power of He^+ at higher M_S is to use heavier projectile ions.[6] Fig. 2 contains plots of the scattering energy for He^+ and three other noble gas ions: Ne^+, Ar^+, and Kr^+ as a function of M_S. These curves were derived directly from eqn (1). It is interesting to note the slopes of these lines. At about M_S = 40 u, the curve for Ne^+ has a higher slope than that for He^+, *i.e.*, the resolving power of Ne^+ becomes higher than that of He^+ at this point. Then, a little over 100 u, Ar^+ shows a higher slope than Ne^+, and finally after about 200 u, Kr^+ has the highest slope. Fig. 3 is a plot of the energy difference per nominal mass *vs.* M_S, *i.e.*, it is the plot of the slopes (derivatives) of the curves in Fig. 2. Note that the plot does indeed show He^+ being the most effective probe up to $M_S \sim 40$ u, followed by Ne^+ up to $M_S \sim 100$ u, *etc.* Thus, in general, LEIS better resolves heavier atoms with heavier projectiles. This is all consistent with our earlier analogy – imagine how hard it would be to differentiate between 16 lb and 18 lb bowling balls by measuring the backscattering energy of ping pong balls bouncing off of them. Eqn (1) would apply to this classical

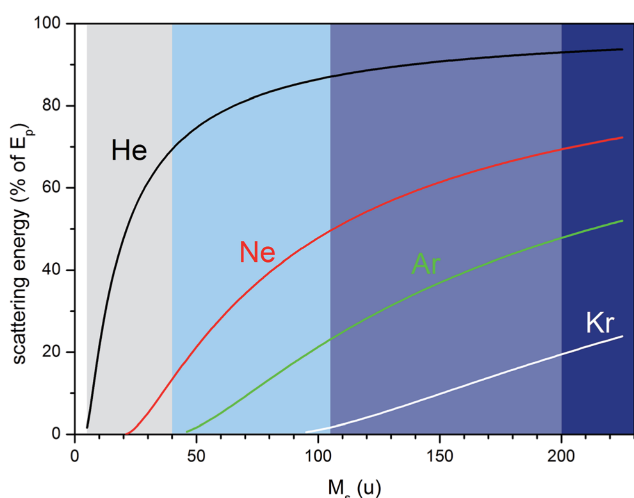

Fig. 2 Percentage of kinetic energy, obtained through eqn (1), retained by the backscattered projectile ion ($E_S/E_P \times 100\%$) plotted as a function of the mass of the analyte atom, M_S. The colored vertical stripes show which noble gas ion is commonly used to probe elements of the corresponding mass range in LEIS.

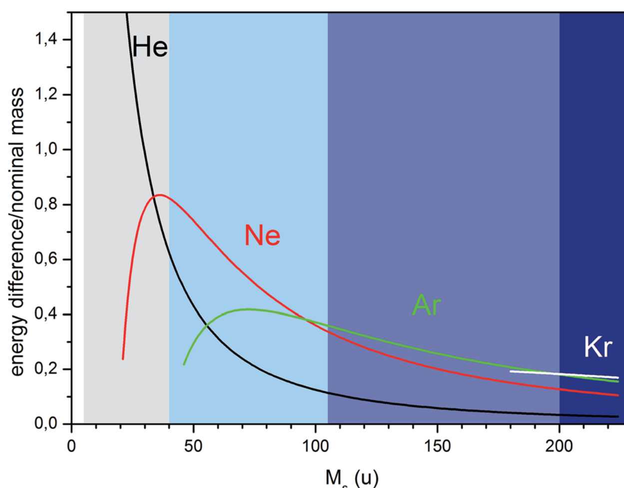

Fig. 3 Plot of energy difference per unit nominal mass *vs.* M_S, *i.e.*, the derivative of the curves in Fig. 2. The colored vertical stripes indicate the noble gas ion that is commonly used to probe elements of the corresponding mass range. The projectile ion that provides the largest energy discrimination per unit mass corresponds to the highest line (curve) at any given M_S in the plot.

Published on 05 April 2016. Downloaded by DTU Library on 4/3/2020 2:12:37 PM.

Published on 05 April 2016. Downloaded by DTU Library on 4/3/2020 2:12:37 PM.

problem, and the mass ratio M_S/M_P would be extremely large, essentially giving the same backscattered energy ($E_S = E_P$, eqn (4)) for the ping pong balls.

Before going on, let's revisit the discussion of LEIS of ^{58}Ni and ^{59}Co. It will illustrate another important concept – consideration of the different isotopes of elements to be analyzed by LEIS. The discussion above on ^{58}Ni and ^{59}Co was true for isotopically pure samples of these elements. However, a real sample of nickel will consist primarily of ^{58}Ni (68.1%) and ^{60}Ni (26.2%). ^{59}Co, in contrast, exists as one stable isotope. It has an odd number of protons (27) so one would expect it to have fewer isotopes than nickel, which has an even number of protons (28). All of this means that a real sample of nickel will produce a broader LEIS signal than the corresponding signal from Co. Accordingly, detecting a small amount of Co in a sample of Ni by LEIS is a difficult proposition – the Co signal lies between the two Ni signals. In contrast, a small amount of Ni in Co can be more readily detected and quantified – the nickel will produce a lower, broader signal that will surround the sharper signal from the Co. We emphasize here that it would be a good idea to perform LEIS in conjunction with other analyses. In this regard, LEIS is the same as any other surface/material analytical method. For example, because of the overlap between the Ni and Co signals, it might be a good idea to perform XPS on any samples that are suspected of containing these two elements. XPS might show, for example, that one of these elements is absent, which would simplify one's data analysis. Of course, as mentioned above, XPS probes much deeper into materials than LEIS.

We now discuss the energy of the backscattered ion and its impact on signal. We noted above that the slope of the scattering energy in Fig. 2 changes with increasing M_S. We also noted that the energy difference between He^+ backscattered from isotopically pure ^{58}Ni and ^{59}Co was 10 eV for the given conditions. In contrast, the energy differences for 5 keV Ne^+ and 8 keV Ar^+ backscattered at 145° from ^{58}Ni and ^{59}Co are 33.1 and 30.3 eV, respectively. There is little difference between these energies, so one might assume that it does not matter whether one uses 5 keV Ne^+ or 8 keV Ar^+. However, the average backscattering energies (kinetic energies) for these ions are *ca.* 1363 and 365 eV, respectively. Thus, the Ne^+ ion is moving much faster than the Ar^+ ion. As a consequence, the Ne^+ ion will have a much shorter interaction time with the surface than the Ar^+ ion during backscattering. This longer interaction time for Ar^+ gives it more time to be neutralized and thus the LEIS signal of Ar^+ backscattering off of ^{58}Ni and ^{59}Co is greatly reduced. This shows that, in addition to selecting the projectile ion that maximizes mass resolution, its effect on signal amplitude must be taken into account. Therefore, the energy of the backscattered ion in LEIS is another important factor to consider in optimizing an experiment.[6]

LEIS is primarily considered to be a surface analysis technique, and this is arguably its greatest strength. Nevertheless, scattering from deeper layers occurs and provides additional important information. The information depth for LEIS is 5–10 nm. LEIS is unique in its ability to nondestructively provide depth resolved information over this range, yielding much higher depth resolution than RBS.[6,8] Because this depth profile is obtained without the need for sputtering, it is often called a static depth profile. Of course, sputter depth profiling is performed in both XPS and ToF-SIMS, but the corresponding sputtering process can rapidly scramble the composition of the outermost layers. Fig. 4a illustrates the interesting mechanism by which static depth profiling information is obtained in LEIS. For a surface scattering event like the one illustrated in Fig. 4a to be detected, the incident ion cannot be neutralized when it is scattered. However, when a noble gas ion enters a solid it is neutralized and travels through the solid in this uncharged form. As it moves along, it loses energy due to electronic and nuclear stoppage events. At some point, a backscattering event may occur, which reverses the trajectory of the atom and directs it out of the solid. In its neutral state, the projectile will not be detected by the instrument. Fortunately, when neutral noble gas atoms leave a solid, a fraction of them are reionized. But unlike most of the processes considered to this point, which can be explained by classical physics and are independent of chemical bonding or other such complexities, this reionization depends on the surface chemistry of the sample. For example, due to resonance between the core electron levels of He atoms and oxygen atoms, oxygen is particularly effective at reionizing helium atoms as they leave the surface of a sample. Therefore, the magnitude of the depth signal tends to scale with oxygen concentration at the outer surface of a sample.[6] Backscattering from atoms that are below the surface results in the long, relatively flat tails/steps present in Fig. 4. The depth of an analyte within a material corresponds to the lengths of these tails. More specifically, the lengths of these tails can be converted to physical depths within the sample if the energy loss per depth interval (eV nm^{-1}) is known for the energy used. This can either be measured directly from known samples or calculated by use of modeling software for ion implantation such as TRIM/SRIM.[17–19] Software for analyzing RBS data has also been successfully applied to LEIS static depth profiles.[20]

Fig. 4b shows the theoretical LEIS spectrum for the ZrO_2 film on Si shown in Fig. 4a. The tall, sharp Zr_{surf} peak at high energy in the spectrum confirms the presence of this element at the outermost surface of this sample. This sharp signal shows a flat tail, labeled Zr_{depth}, towards lower energy. In accord with the previous discussion, this tail is due to ions that have entered the solid, been neutralized, undergone backscattering (by Zr atoms), and been reionized during their emission from the solid. Their reionization was favored because ZrO_2 is an oxide. Obviously deeper Zr atoms in the film correspond to signal on the tail that is further from the Zr_{surf} peak. Below this tail for Zr is an arrow pointing to where the signal for silicon would appear if silicon atoms terminated the material. They do not, and no signal is observed here. The next lower signal in energy labeled O_{surf} is from surface oxygen atoms. The presence of this peak and the Zr_{surf} peak confirm that this solid is terminated with these atoms. Finally, there is a step labeled Si_{depth}. This signal is due to backscattering from silicon atoms below the ZrO_2 film. Notice that unlike the Zr_{surf} and Zr_{depth} signals that are fused together in Fig. 4b the hypothetical Si_{surf} and real Si_{depth} signals are separated in energy because of the presence of the ZrO_2 film.

 This journal is © The Royal Society of Chemistry 2016

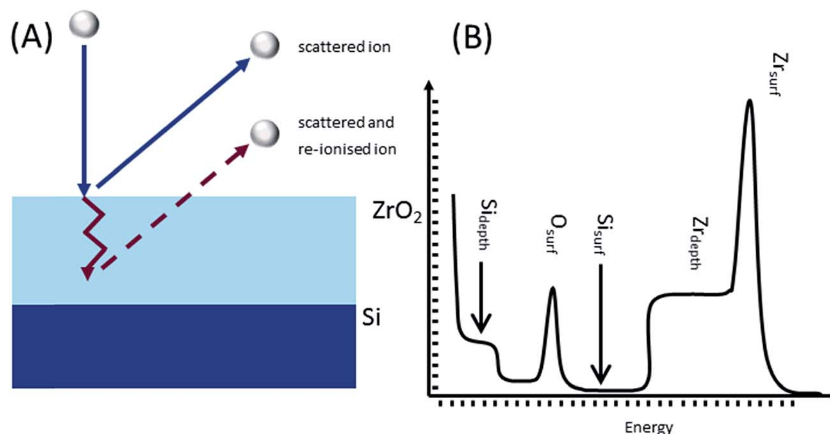

Fig. 4 (A) Noble gas ion scattering off of a ZrO_2 film on Si. Shown are: (i) ion scattering from the surface, and (ii) particle penetration, neutralization, backscattering, and reionization. (B) Mock LEIS spectrum for the material shown on the left. Figure was modified from its original form, but also used with permission from: 'Surface Microanalysis by Low-Energy Ion Scattering' in *Microscopy Today*, Vol. **19**, Issue 02, Mar. 2011, pp 34–38 by T. Grehl, E. Niehuis and H. H. Brongersma.

Published on 05 April 2016. Downloaded by DTU Library on 4/3/2020 2:12:37 PM.

One of the best ways to come to understand a new technique is to study the real data it produces. Accordingly, in Fig. 5 we show a series of real LEIS spectra from the atomic layer deposition (ALD) of ZrO_2 onto silicon. ALD is a technique for producing highly conformal thin films, and films deposited by ALD are very relevant to semiconductor manufacturing.[21–24] Each ALD cycle here consists of the appropriate two half reactions. These surfaces were cleaned with atomic oxygen prior to analysis, and therefore the outermost layer of the material is expected to be fully oxidized. The spectra in question (see Fig. 5) were obtained after 10, 20, 30, 40, 50, 70, and 100 ALD deposition cycles. These real spectra correspond to the idealized representation of this system and LEIS spectrum in Fig. 4. These spectra primarily contain three peaks that are assigned, based on their backscattering energies, to O, Si, and Zr. Qualitatively, the positions of these signals on the energy scale correlate with their mass numbers – Zr is the heaviest atom, which produces the highest backscattering energy, followed by Si, followed by O.

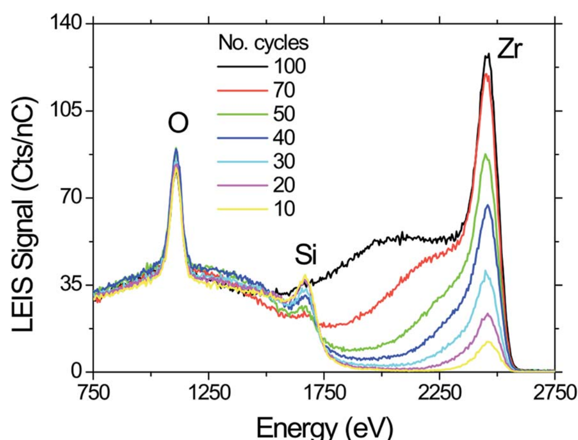

Fig. 5 LEIS spectra for ALD deposited zirconium oxide on a silicon substrate for 10, 20, 30, 30, 50, 70, and 100 cycles.

All of this is reasonable. The signal from the Si substrate is initially rather intense, and it has a tail (high background) to lower energy that corresponds to signal from subsurface atoms. The fact that there is *any* signal from the Si substrate is quite interesting. The idealized view of ALD is that it creates perfectly uniform and conformal layers on a substrate, *i.e.*, one might argue that under ideal conditions even a small handful of ALD cycles should completely cover the substrate with ZrO_2. Clearly this is not the case after even 10 deposition cycles. Two possibilities here are (i) that the ALD cycles have led to submonolayer deposition of Zr that is uniformly dispersed across the surface, leaving a significant number of exposed substrate atoms, *i.e.*, not very much material is depositing per cycle, or (ii) that growth of the ZrO_2 is occurring from nucleation sites on this material, which is also leaving a considerable amount of the original surface exposed. Atomic force microscopy or high resolution scanning electron microscopy would help elucidate the actual surface structure. Again, the multi-instrument characterization of materials is often important for these types of problems.[25–27] For now, it is enough to know that LEIS has suggested that some rather interesting complexity is present in this ALD deposition.

The general trends in the peak intensities in Fig. 5 are consistent with the ALD deposition of ZrO_2. The substrate peak, labeled 'Si', gradually decreases in intensity with increasing number of deposition cycles, which is perfectly consistent with another material gradually covering the substrate. At the same time, the Zr signal is increasing in intensity, *i.e.*, the expected deposition and increasing surface coverage of ZrO_2 is occurring. Interestingly, the oxygen signal stays nearly constant throughout these depositions, suggesting that its surface concentration stays nearly constant. This is reasonable because the samples were all treated with atomic oxygen prior to analysis. This result is also consistent with oxygen in SiO_2 at the surface being replaced with oxygen in ZrO_2, such that the oxygen concentration at the surface stays roughly constant. As the Zr signal increases in intensity, the tail to its low energy side also increases in intensity. At 100 deposition cycles, this tail is

initially flat, suggesting a uniform concentration of Zr to some depth below the surface. The length of the tail corresponds to a thickness of about 2.5–3 nm of ZrO_2. The tail then decreases in intensity, which suggests that lower in the film the concentration of Zr has decreased. At 100 deposition cycles, the Si signal is finally gone – all the silicon surface atoms are covered. Quite a few ALD cycles were required to completely cover the substrate. These results are consistent with ZrO_2 growth from nucleation sites, *i.e.*, growth here does not take place as perfectly homogeneous, uniform layers but from select locations. In summary, the real spectra in Fig. 5 correspond to the rather complex, and interesting, deposition of ZrO_2. It is clear how valuable the remarkable surface sensitivity of LEIS is in this problem.

Finally, we see in Fig. 5 another analogy between LEIS and RBS. Like LEIS, in RBS incoming projectile ions scatter with greater energy from heavier atoms. Thus, an ideal situation in RBS is the analysis of heavy atoms on a light substrate because the signal from the heavy atoms will be well separated from the substrate signal and most easily analyzed/quantified.[26] These signals often have little or no noise around them. Note that we have this situation for the Zr signal, especially for lower numbers of deposition cycles.

3. LEIS instrumentation[28]

As noted above, LEIS has been in use since the late 1960's. However, recent developments have dramatically improved its sensitivity and applicability.[1,6] Here, we discuss some of the basics of LEIS instrumentation, including recent advances in instrument design. The main components of a LEIS instrument are a noble gas ion source and an energy analyzer/detector for measuring the energies of backscattered particles and for quantifying this signal. Obviously, ion optics are needed to control the incoming ion energy, to focus the probe beam, and to set the pass energy into the kinetic energy analyzer. LEIS analysis takes place under ultra-high vacuum conditions, requiring a vacuum chamber with associated pumps, gauges, and load-locks. Given the extreme surface sensitivity of LEIS, sample preparation is of vital importance. Many LEIS instruments include a sample preparation chamber in which samples are cleaned, cleaved, heated, and/or treated with various gasses to simulate the operating conditions of the materials being analyzed. If the samples cannot be prepared *in situ*, the preferred type of cleaning in LEIS is treatment with atomic hydrogen or oxygen. These species can remove surface contamination without causing sputter damage. In comparison, sputter cleaning and plasma cleaning bombard a surface with high-energy particles, which causes some degree of material removal and surface rearrangement.

The most common type of LEIS instrument is a converted XPS instrument. The electrostatic analyzers (ESA) commonly used in XPS measure the kinetic energies of surface-emitted photoelectrons. To use an ESA for LEIS it is only necessary to reverse its polarity to accommodate particles with positive charges. A hemispherical ESA configured for LEIS analysis is shown in Fig. 6. Here, the two main components are a set of ion optics that set the pass energy, and a pair of concentric hemispheres with applied voltages. Incoming ions with too little energy collide with the negative hemisphere, while ions with too much energy collide with the positive hemisphere. Only ions with the correct pass energy maintain a stable trajectory through the analyzer and reach the detector.

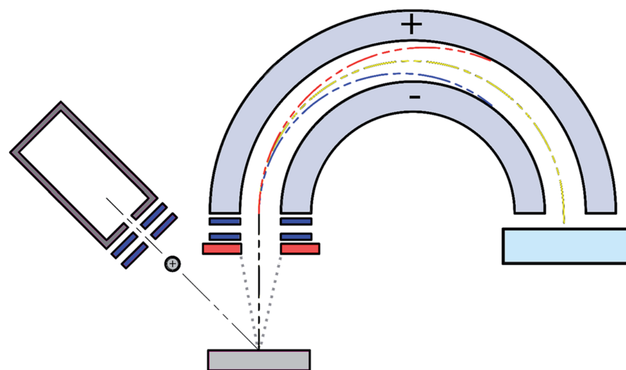

Fig. 6 Representation of a converted XPS instrument for LEIS analysis. The angle of acceptance permitted by the entrance slits of the hemispherical ESA is represented by a pair of dotted, grey lines. The trajectories of ions with too much energy (red), too little energy (blue), and the correct amount of energy (yellow) are shown.

The advantage of using a converted XPS instrument for LEIS analysis is that for the additional expense of installing a noble gas ion source, a single instrument can serve both functions. However, the geometry of a hemispherical ESA only allows the capture of a small fraction of the total number of backscattered ions. Since the goal in LEIS is almost always to analyze the outermost layer of the material, and the surface can only take a limited ion dose before surface damage from the probe beam influences the analysis, the entrance apertures of the ESA are usually opened to the maximum amount possible to achieve sufficient sensitivity. This results in a spread of several degrees in the accepted backscattered angle, Θ, represented by the dotted lines above the sample in Fig. 6. As indicated in eqn (1), the energy of backscattered particles depends on Θ, so a spread in Θ results in peak broadening and concomitant loss of mass resolution. For example, using 3 keV He^+ ions at a scattering angle of 145° and a spread in the angle of $\pm 5°$, the peak for ^{65}Cu is broadened by 29 eV. This corresponds to the difference in scattering energy separating Cu and Zn (it is nominally 24 eV), so their identification becomes challenging. As discussed in the previous section, heavy elements are often analyzed with heavier projectile ions. If we tried to resolve Cu and Zn using this same instrumentation, but with 5 keV Ne^+ ions as the probing beam, the nominal spacing between these signals increases to 88 eV. This is positive. Unfortunately, however, we get an energy spread of 98 eV from the angular spread in Θ. Obviously this difference is large enough that it is again challenging to distinguish these neighboring peaks, especially when other sources of peak broadening are taken into account. For heavier elements, the effect of peak broadening by the wide acceptance angles employed in converted XPS instruments is even more pronounced. Thus, LEIS instruments derived from XPS systems are usually used only with He^+ ions and are not well suited for resolving analytes of high nuclear mass.

Published on 05 April 2016. Downloaded by DTU Library on 4/3/2020 2:12:37 PM.

 This journal is © The Royal Society of Chemistry 2016

Published on 05 April 2016. Downloaded by DTU Library on 4/3/2020 2:12:37 PM.

Even with a wide acceptance angle, a high ion dose may still be required to achieve a good signal-to-noise (S/N) ratio in a converted XPS instrument, resulting in sample damage. That is, the first ions to backscatter from a region provide information about the pristine surface. However, any ions that strike a sputtered region will provide information about the damaged surface. Therefore, an analysis must be performed within the static limit to obtain information about the pristine sample surface. The static limit, which is also an important consideration in ToF-SIMS, is the ion dose below which there is a low probability of the same spot being struck twice. With converted XPS instruments, the sensitivity of the analyzer may not be sufficient to get a good S/N ratio while maintaining an ion dose below the static limit. This obstacle can be overcome by analyzing multiple spots on the same sample, but this approach requires a uniform surface.

The first papers on the double toroidal analyzer (DTA) were published in the 1980s.[4,5,29] This design was refined over the next 20 years,[16] and finally incorporated into a commercial instrument. A schematic representation of a DTA can be seen in Fig. 7. The DTA is similar in function to the hemispherical ESA used in XPS; in both cases, only an ion of the correct kinetic energy can traverse the space between two charged plates without colliding with one of them. With this geometry, the probe beam strikes the sample vertically, and a nearly 360 degree azimuth of backscattered ions is collected. With this large azimuthal collection angle, it is possible to sample a very narrow range of backscattering angles, Θ, while still collecting a much larger number of ions than with a hemispherical ESA. The typical spread in Θ for an analysis with a DTA-equipped instrument is 1–2°, which clearly results in much less peak broadening than with a hemispherical ESA instrument. Accordingly, instruments with DTAs are suited for use with all types of noble gas ions, not just He^+, and practically all pairs of elements can be separated.[30] Thus, DTA equipped instruments can achieve much lower detection limits before the static limit of analysis is reached. ION-TOF has commercialized this technology in their Qtac^{100} system, which is a dedicated LEIS instrument. In addition to incorporating a DTA into their design, ION-TOF has introduced other features that further improve the performance of the instrument. The first that bears mentioning is a position sensitive detector. As shown in the Fig. 7, the DTA can simultaneously pass ions of a range of energies (5–10% of the pass energy). Ions of different energies have different trajectories through the analyzer. Thus, they strike the position sensitive detector plate at different positions, so that their individual energies are determined based on the position at which they strike it. This arrangement has the advantage of accepting a higher scattered ion flux without loss of energy resolution. Similar technology has long been available for use with hemispherical ESAs, but a considerable amount of engineering was required to make a position sensitive detector compatible with the DTA geometry while covering a wide energy range of parallel detection. Another feature included in the instrument is time-of-flight-filtering (ToF-filtering), which allows the backscattered projectile ions to be isolated from sputtered background ions of the same energy. The most abundant background ion in any LEIS analysis is from adsorbed hydrogen that has been sputtered from the sample and ionized in the sputtering event. These secondary hydrogen ions may have the same kinetic energies as backscattered noble gas ions. However, their lower mass gives them a much higher velocity resulting in a much shorter time-of-flight. Therefore, by

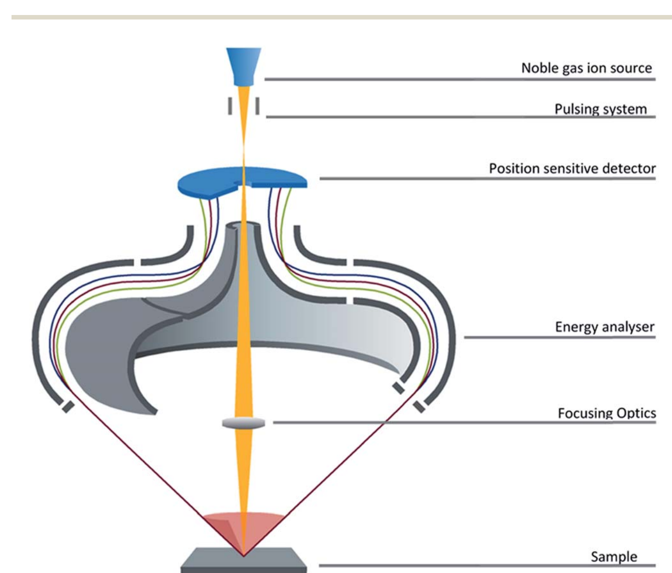

Fig. 7 Schematic representation of a double-toroidal analyzer, as included in the Qtac^{100} instrument by ION-TOF. Figure was modified from its original form, but also used with permission from: 'Surface Microanalysis by Low-Energy Ion Scattering' in *Microscopy Today*, Vol. **19**, Issue 02, Mar. 2011, pp 34–38 by T. Grehl, E. Niehuis and H. H. Brongersma.

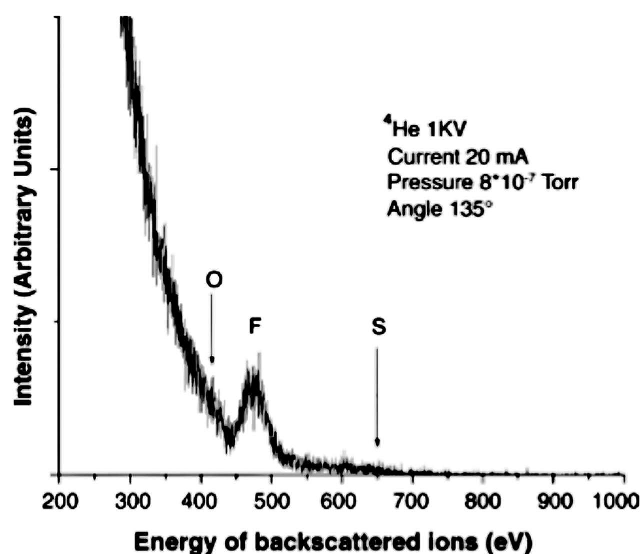

Fig. 8 LEIS spectrum taken with a conventional XPS instrument using a 1 keV $^4He^+$ ion beam. Reprinted from 'X-ray photoelectron spectroscopy and low energy ion scattering studies on 1-buthyl-3-methyl-imidazolium bis(trifluoromethane) sulfonimide' by S. Caporali, U. Bardi, and A. Lavacchi in *Journal of Electron Spectroscopy and Related Phenomena*, **151** (2006), 4–8, Copyright 2005, with permission from Elsevier.

View Article Online

Published on 05 April 2016. Downloaded by DTU Library on 4/3/2020 2:12:37 PM.

detecting only ions with the correct flight time for each energy, this background signal can be eliminated. This is especially beneficial in the low-energy region of a LEIS spectrum, where the background signal can be strong enough to obscure the peaks of the light elements.[9] For example, Fig. 8 shows a LEIS spectrum taken with a conventional XPS-based instrument.[31] The very high background at lower scattering energies is obvious. These advances in LEIS instrumentation have dramatically improved the sensitivity and applicability of this technique to a variety of samples.

4. A photographic tour of the Qtac^{100}, a double-toroidal analyzer-equipped LEIS instrument[32]

Fig. 9 shows a Qtac^{100} LEIS instrument with the locations of a few key components labeled. Clearly, a LEIS instrument will require an ion source (A), a gun for accelerating the ions (B), and an energy analyzer (top of the main chamber, (D)). In addition, instruments can be equipped with sputter guns (C) for depth profiling. In LEIS, ions must travel rather long distances without colliding with other atoms besides those at the sample surface, *i.e.*, have long mean free paths. Thus, LEIS is carried out under ultra-high vacuum (UHV) conditions. Fig. 9 also shows some of the key components that are necessary for UHV analysis. These include the analysis chamber (D) – these kind of look like divers' helmets, a sample introduction chamber (E, load lock), and a sample manipulator (transfer arm) (F) to move samples from the load lock to the UHV analysis chamber. Almost all UHV analysis systems have this type of two-chamber design – an introductory chamber and an analytical chamber. The purpose of this important design feature is to reduce contamination in the main chamber so that pump down times are not excessively long. The vacuum pumps for the system are housed beneath the analysis chamber (G), which is typical of many UHV surface analytical instruments.

Fig. 9 LEIS Qtac^{100} instrument with locations of key components labeled. (A) Ion source. (B) Ion gun. (C) Sputter gun for depth profiling. (D) Analysis chamber (the double toroidal analyzer is located at the top of this chamber). (E) Sample introduction chamber (load lock). (F) Sample manipulator (transfer) arm. (G) Vacuum pumps and other hardware are housed below the instrument.

Obviously a LEIS system can be configured with/connected to other analytical instruments. Fig. 10 shows a combined LEIS/ToF-SIMS instrument. The main chambers of the two instruments are connected so that samples can be transferred from one instrument to the other without breaking vacuum. Clearly this capability (i) adds noticeably to the cost of the instrument, but (ii) allows sample analysis at a level that is not possible if the material must come in contact with the air prior to or between analyses.

Fig. 11 shows the sample preparation and loading process for the Qtac^{100}. Because of the extreme surface sensitivity of LEIS, sample cleanliness is very important. Gloves are used for handling samples and the sample holder. We note the irony that gloves are worn in most chemistry laboratories to protect the workers from chemicals, while gloves are worn in most surface analysis labs to protect the samples and instruments from humans! Samples with dimensions of *ca.* 15 mm × 15 mm fit on these sample holders, and depending on the instrument configuration, one or several samples may be loaded at a time. The sample holders connect to a holder pen for easy handling. Because of LEIS′ surface sensitivity, adventitious carbon can quickly reduce or eliminate surface signals. The adventitious hydrocarbon typically gives no signal since it is often H-terminated, and LEIS is not sensitive to hydrogen. Accordingly, atomic oxygen or hydrogen cleaning is a common step in sample preparation, where each sample may require a different cleaning time. The samples are typically given increasing doses of atomic oxygen until a stable instrument response is obtained. An optional feature for the Qtac^{100} is an environmental chamber in which samples can be heated, cooled, and/or dosed with different gasses. Single-sample sample holders are practical in LEIS because each sample may need different cleaning times or undergo different treatments in the environmental chamber.

Fig. 12 shows a close-up view of a Qtac^{100} instrument with some key components labeled. This particular instrument is configured to hold multiple sample holders simultaneously. It also has the optional environmental chamber. Identified in this picture are the atomic oxygen generator (A), a sputter gun for

 This journal is © The Royal Society of Chemistry 2016

Published on 05 April 2016. Downloaded by DTU Library on 4/3/2020 2:12:37 PM.

Fig. 10 ToF-SIMS 5 and Qtac[100] instruments (left and right, respectively), with their main chambers connected.

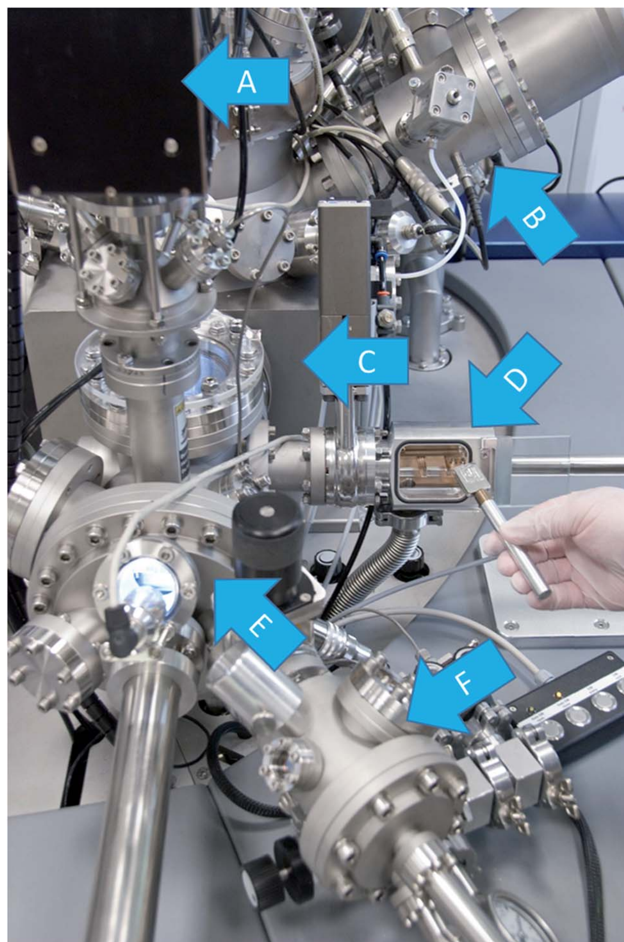

Fig. 12 Close-up view of the Qtac[100] instrument at IONTOF with selected components labeled. (A) Atomic oxygen generator. (B) Sputter gun. (C) Analytical (main) chamber (cube). (D) Sample introduction chamber. (E) Sample preparation chamber. (F) Environmental chamber.

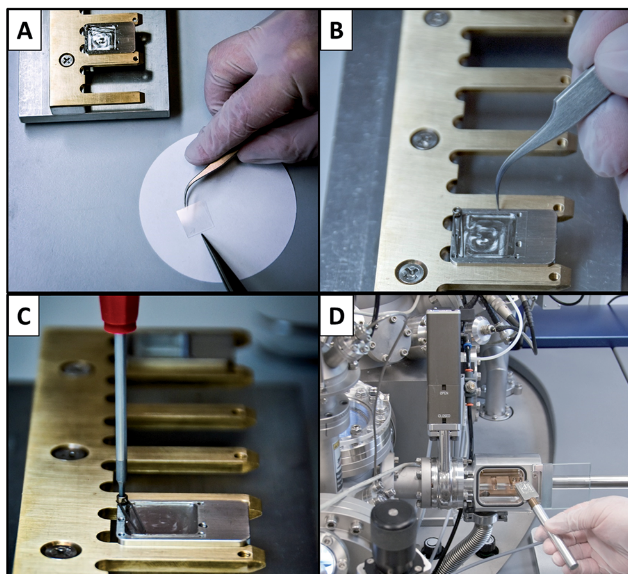

Fig. 11 Sample loading process for the Qtac[100]. (A) Glass sample, handled with tweezers and gloves. (B) Placing the sample on the holder (silver colored). (C) Securing the sample to the holder with a spring clip. (D) Sample transfer to the load lock while handling the holder with a special sample-holder pen.

sputter depth profiling (B), the analytical (main) chamber (C), the sample introduction chamber (D), the sample preparation chamber (E), and the environmental chamber (F). Three separate transfer arms are visible in this picture – they move samples between the various chambers. Note the small size of the sample introduction chamber on this instrument. Small introduction chambers make for faster pump downs and help minimize contamination of the analytical (main) chamber. Fig. 13 shows a screenshot of the instrument software. Practically all of the instrument components are controlled through this software, which includes tools for peak fitting spectra.

5. Quantitation in LEIS[33]

We now discuss the quantitative nature of LEIS, why LEIS is inherently quantitative, and how quantitation is accomplished in LEIS. We also mention some of the few cases in which LEIS is not quantitative.

Published on 05 April 2016. Downloaded by DTU Library on 4/3/2020 2:12:37 PM.

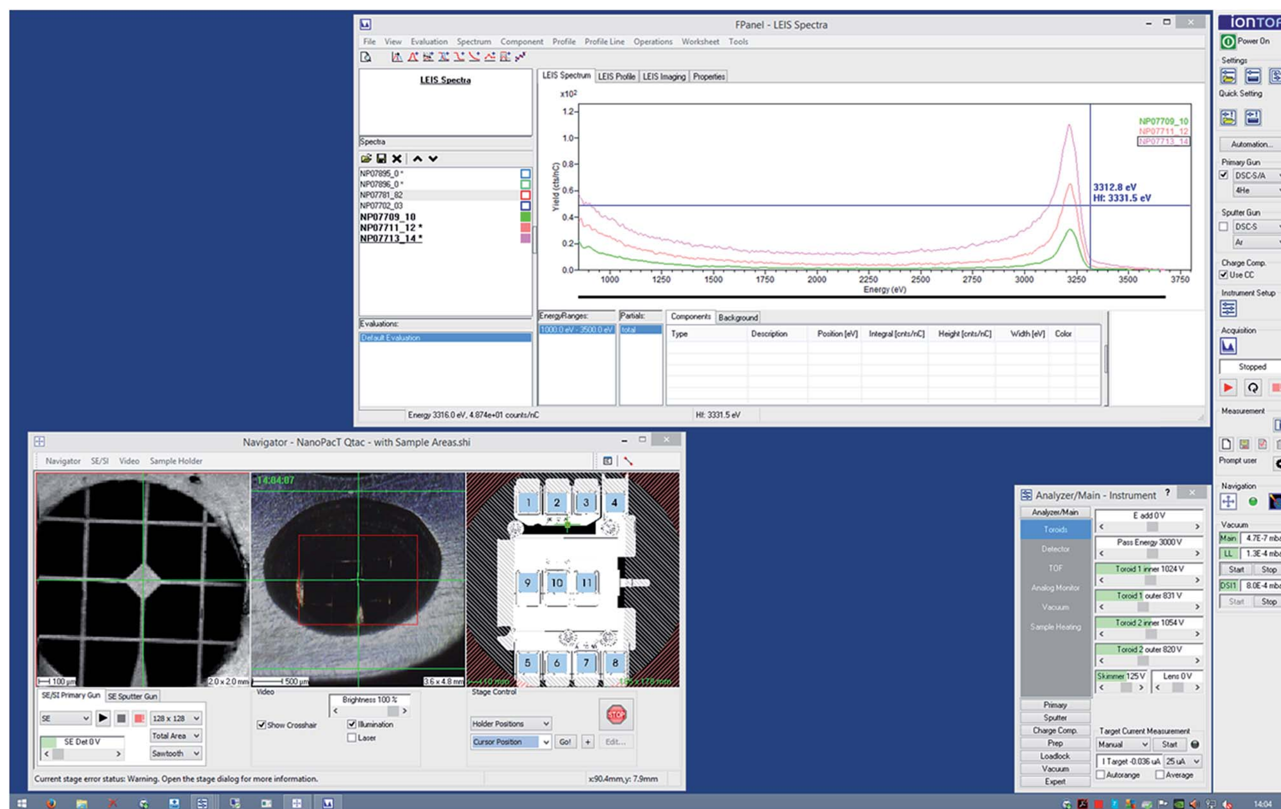

Fig. 13 Screenshot of the Qtac[100] instrument software. Data collection window (Top). Stage control window (Bottom left). Instrument setting window (Bottom right). Instrument controls (far right).

LEIS is inherently quantitative.[6] Thus, unlike ToF-SIMS, there is no matrix effect, with a few exceptions that will be noted below. The governing equation of LEIS (eqn (1)) is derived entirely from classical principles, where this process (essentially the ricochet of a lighter particle off of a heavier one) occurs independently of the chemical environment of the analyte ion. However, a factor that influences the backscattered intensity is the probability of the ion being neutralized during the scattering event. Recall that the analyzer only detects ions, not backscattered neutrals. Because neutralization effects are dominated by the binary interaction between the ion and the analyte atom, and because of the relatively high energy and short interaction time of the collision, the chemical environment of the atom and/or the state of the surface as a whole is irrelevant. Because there is no matrix effect, the signal in LEIS is directly proportional to the surface coverage of elements, which makes quantitation straightforward. In contrast, the strong matrix effect in ToF-SIMS causes signals of certain ions to be enhanced or suppressed depending on which other atomic species/compounds are present. In some cases, this can be used advantageously to enhance certain signals, or most of them, as in metal assisted SIMS (MetA-SIMS).[34–36] However, it also means that for most circumstances ToF-SIMS is at best semi-quantitative. While there is no matrix effect in LEIS, each element has its own sensitivity factor. In this regard it is analogous to XPS. Indeed, each element has a unique LEIS backscattering cross-section and also a neutralization cross-section. These vary depending on the projectile ion and projectile energy used. While scattering cross sections can be calculated, there is currently no computational model for predicting neutralization cross sections, and in practice sensitivity factors are established empirically, either by the use of standards or correlation plots.[6] In some sense this is the same as in ToF-SIMS, where the sputtering process is quite well understood and can be modelled by molecular dynamics simulations, while the ionization effects are still not possible to predict.

The data in Fig. 14A illustrate the absence of a matrix effect in LEIS. These data were collected from tungsten surfaces onto which different amounts of bromine were adsorbed. The signal for tungsten is plotted on they *y*-axis, and the signal for bromine is plotted on the *x*-axis. Because LEIS measures atomic surface coverages, as the surface coverage for bromine increases, we should see a decrease in the tungsten signal, and *vice versa*. This is exactly what the data show. When the tungsten signal is high, the bromine signal is low, and *vice versa*. The fact that there is no matrix effect is proved by the linear, anticorrelated relationship shown here. If there were a matrix effect, we would see a departure from these linear trends. For example, if bromine had a suppressing effect on the tungsten signal, we would see the tungsten signal increase in a non-linear fashion as the bromine concentration decreased. Numerous experiments with other two-component systems have shown similar results. For example, Fig. 14B shows the steady increase in the LEIS Zr signal in the atomic layer deposition (ALD) of ZrO_2 onto SiO_2

This journal is © The Royal Society of Chemistry 2016

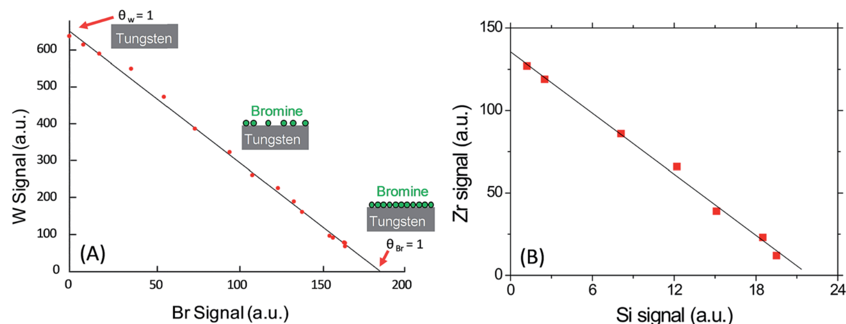

Fig. 14 (A) Results from a LEIS analysis in which bromine was adsorbed *in situ* onto a tungsten substrate under different conditions. (B) Results from a LEIS analysis of a series of samples with increasing amounts of ZrO_2 deposited on SiO_2 by atomic layer deposition (ALD). In both cases, the resulting linear relationship between the signals shows that the technique is free of any matrix effect.

Published on 05 April 2016. Downloaded by DTU Library on 4/3/2020 2:12:37 PM.

with the expected, concomitant decrease in the Si signal. Besides serving as a proof that there is no matrix effect, the anticorrelation plots in Fig. 14 are also used to obtain the sensitivity factors for the analytes. When such a plot can be constructed, the signal for 100% surface coverage of each analyte can be obtained by extrapolating to the axes. For the example of W/Br system shown in Fig. 14A, the signal for the 100% tungsten surface coverage is about 650 arbitrary units, and the signal for 100% bromine surface coverage is at about 180 arbitrary units.

Correlation plots are useful when two (or sometimes three) components in a series of samples vary in coverage.[37] In those cases, the sensitivity factors can be determined without knowledge of any of the sample surface compositions and without pure reference materials. However, samples with many analytes require the use of standards. Pressed oxide powders are the most commonly used reference materials in LEIS. Many samples of interest are oxides, so oxide powders are a natural choice for these applications. Furthermore, samples are often cleaned with atomic oxygen in preparation for LEIS analysis, and samples cleaned in this way will have their outer surfaces oxidized, again making oxide powders a good choice as standards. Most metal oxides are oxygen-terminated, and the metal atoms in the structures are shielded to some degree by oxygen atoms. In these cases, *e.g.*, the samples illustrated in Fig. 14B, the metal signal is taken to be representative of the metal oxide coverage. For example, if pure zirconium oxide powder gives a Zr signal of 100 counts for a given set of analysis conditions, then a sample that yields a signal of 50 counts will have a surface coverage of 50% ZrO_2. LEIS is largely insensitive to surface topography, so the inherent roughness of a pressed powder standard poses no problems. One notable advantage that powders have over their bulk counterparts is that they tend to dilute surface contamination. Contaminants often diffuse to the outside of a material to minimize surface energy. Since bulk materials have low specific surface areas (surface area per unit mass), contaminants can become concentrated at their surfaces. For example, a 1 mm thick sample has on the order of 5×10^6 atomic planes. If the bulk concentration of a contaminant is 0.2 ppm, there are enough atoms of the contaminant to form a complete layer on the surface, provided all the contaminant atoms are mobile. Powders, with their much higher specific surface areas, tend to dilute these contaminants. Of course, not all samples are oxides. When metals are analyzed, pure metals can be used as standards, although some degree of sputtering may be necessary to remove the native oxide layer. In principle, any material having a known coverage of the element of interest and being reasonably easy to prepare is suited as a reference, *e.g.*, PTFE (Teflon) for fluorine.

There are some circumstances in which LEIS may be subject to a matrix effect. Most often, these occur in situations where the model of a purely binary, inelastic collision interaction between two particles no longer applies. One such example is the difference in sensitivity factor between sp^2 and sp^3 hybridized carbon.[38] The difference in response here is a result of resonant charge exchange between the partially occupied 1s level in the He^+ ion and the filled valence band of graphitic carbon. For sp^3 carbon, this additional source of neutralization does not exist, so the sensitivity factor is significantly different. In some cases, this effect can be turned into something useful. By using this difference and its dependence on the primary energy, graphitic and sp^3 carbon can be distinguished. There may also be tunneling between the partially occupied level of the noble gas ions and the valence band of the material being analyzed – for materials with low work functions, only a small energy barrier must be tunneled through by an electron to neutralize the ion. Since this no longer is a binary interaction, but rather an interaction between the ion and the whole surface, quantification is difficult. Typically, these cases depend on the nature or energy of the projectile, and these matrix effects can be detected or even overcome by changing the primary ion beam energy or the projectile ion used.

In summary, the principle strength of LEIS is that it provides quantitative information about the outermost atomic layer of a material. In general, LEIS has no matrix effect – it is inherently quantitative; its signals are directly proportional to surface coverage. Quantitation in LEIS can be accomplished either with reference samples or, for simple systems where multiple samples are available, by way of a correlation plot. Standards are often chosen based on the goal of the analysis. If the goal is to quantify the concentration of an oxide, oxide powders are used,

Published on 05 April 2016. Downloaded by DTU Library on 4/3/2020 2:12:37 PM.

while metals are used when metallic samples are probed. With the resulting quantitative information, materials for which performance strongly depends on surface composition can be understood at a deeper level.

6. Comparison of LEIS to other surface analytical methods[39]

Table 1 compares the attributes of LEIS, ToF-SIMS, and XPS. Of course, ToF-SIMS and XPS are two of the most commonly used surface analysis techniques for probing the surface chemistry of materials. Indeed, for years, XPS and ToF-SIMS have been used in tandem for surface analysis because of their powerful complementarity. We have written on XPS and ToF-SIMS a number of times in recent tutorial articles in Vacuum Technology and Coating,[40–42] and in our papers.[43–47]

As Table 1 shows, LEIS is more surface sensitive than the other two techniques, which are already very surface sensitive. LEIS acquires static depth profiles (see below) in a more natural way than XPS, and ToF-SIMS does not have this capability. LEIS can also be used to acquire dynamic depth profiles in the same way as ToF-SIMS and XPS, *i.e.*, in conjunction with a sputter gun. Its analysis time is very fast (minutes), which is generally faster than for XPS and comparable to the acquisition time for ToF-SIMS. Its detection limits are generally poorer than those for ToF-SIMS (extremely low) and XPS (moderately low), especially for lighter elements like boron. However, to be fair to LEIS, XPS averages its signal over 10–20 atomic layers, while LEIS only gets its signal from the outermost layer. Therefore, with regards to the detection limit from the outermost atomic layer, LEIS is more sensitive than XPS. LEIS has essentially no matrix effect – in this regard it is more similar to XPS than ToF-SIMS. Of course, ToF-SIMS shows a significant matrix effect, which is one of its disadvantages. Like XPS, one of LEIS' greatest strengths is that it gives quantitative results. This is in contrast to the limited quantitative information that is usually available from ToF-SIMS. LEIS does not give oxidation state information about elements at surfaces, while XPS provides this information in a direct way,[47] and ToF-SIMS does so indirectly. In addition, LEIS does not provide molecular information about surfaces, while ToF-SIMS does so in a direct way and XPS gives it indirectly. The lateral resolution of ToF-SIMS (micron to submicron) is the highest of the three techniques, and those of LEIS and XPS (*ca.* 10 μm) are similar. The cost of the instrumentation for all three techniques is quite high. Perhaps a fair concluding statement would be to say that while no surface analytical technique can provide all of the information one might desire about a surface, LEIS, ToF-SIMS, and XPS are clearly complementary so that they can provide powerful surface and material characterization when used together. A clear advantage of employing all three techniques is that they probe materials at different depths. In summary, it is clear that LEIS has significant capabilities that neither XPS nor ToF-SIMS has. We are confident that in the future we will see more surface analyses that employ all three techniques.

7. Static depth profiling in LEIS[39]

Obviously, LEIS is not the only technique that can provide depth profile information about the outer *ca.* 10 nm of a material. Angle resolved XPS (AR-XPS) can also yield this information without the need for sputtering. However, it is generally difficult to obtain quantitative depth information from AR-XPS data. That is, AR-XPS analyses are usually valuable in a qualitative to perhaps semi-quantitative way, but more precise information requires modeling, which can be challenging.[48] Thus, the static depth profile information provided by LEIS, which is obtained in a more direct fashion, is especially useful for very thin films, *e.g.*, in semiconductor devices. It provides better depth resolution than AR-XPS, where the depth resolution in LEIS is high (0.2–1 nm, depending on sample composition).[14] The interpretation of LEIS depth signals is probabilistic – it depends on the number of possible paths a particle can take to get to and from a certain depth. Obviously, this number increases with depth.

Table 1 Comparison of attributes of LEIS, ToF-SIMS, and XPS

Properties	LEIS	ToF-SIMS	XPS
Surface sensitivity	Outermost atomic layer	A few atomic layers	*ca.* 5 nm
Static depth profiling	Inherent, *ca.* 10 nm	No	If multiple scans taken at multiple angles (angle resolved XPS), *ca.* 10 nm
Dynamic depth profiling	With sputter gun	With sputter gun	With sputter gun
Analysis time per spectrum	Typically minutes	Typically minutes	Somewhat longer
Detection limits	A few % of a monolayer for the lighter elements, up to 0.1–1% for the heavier elements	ppm	0.1–1% of a monolayer
Matrix effect	Essentially none	Strong	Essentially none
Quantitative results	Excellent	Relatively poor	Very good
Oxidation state information	None	Somewhat, through molecular fragments	Yes
Molecular information	None	Yes, through molecular fragments	Yes, through chemical shifts
Lateral resolution	*ca.* 10 microns	Submicron	*ca.* 10 microns
Cost of instrumentation	High, *ca.* $\$1 \times 10^6$	High, *ca.* $\$1 \times 10^6$	High, *ca.* $\$0.5 \times 10^6$

 This journal is © The Royal Society of Chemistry 2016

Published on 05 April 2016. Downloaded by DTU Library on 4/3/2020 2:12:37 PM.

Thus, the uncertainty on the depth resolution in LEIS is less from signals that originate close to the surface, so thinner films are better resolved than thicker ones. LEIS static depth profiles also have clear advantages relative to sputter depth profiles. They avoid the mixing of atomic layers that almost inevitably results when samples are sputtered. This attribute of LEIS static depth profiles has been applied to study diffusion in very thin films.[14,49]

LEIS is a powerful tool for performing sputter depth profiles. This capability is especially useful for thicker samples (up to about 100 nm). Sputter depth profiles in LEIS provide some unique advantages relative to XPS and ToF-SIMS. The first is that the extreme surface sensitivity of LEIS yields a much higher (finer) depth resolution than can be achieved in XPS or ToF-SIMS, provided the sputtering conditions are chosen to keep the atomic mixing low. Second, the quantitation of LEIS surface signals is straightforward. Third, the static depth profile and the sputter depth profile in LEIS provide complimentary information. Ter Veen *et al.* demonstrated that the static depth profile information from an $Si/SiO_x/W/Al_2O_3$ ALD stack provided a useful preview to subsequent sputter depth profiles, making it possible to identify artifacts that result from sputter beam effects.[50] A fourth advantage of combining LEIS and sputter depth profiling is that because many spectra are obtained with varying compositions within the depth profile, sensitivity factors for elements can be obtained without the need for reference materials. This further simplifies the process of using LEIS to obtain quantitative depth profile information. Ter Veen *et al.* explain this method in detail in their article.[50]

8. Application of LEIS to semiconductors[39]

Critical dimensions in semiconductor devices continue to decrease. Therefore, surface sensitivity is becoming an increasingly important attribute for techniques used to analyze thin films in them. A 2006 study by Stokhof and coworkers takes advantage of the extreme surface sensitivity of LEIS to study the nucleation and growth (to closure) of WN_XC_Y films deposited by ALD with the goal of better understanding copper diffusion barrier layers in semiconductor devices.[51] Their article notes that as a consequence of shrinking critical dimensions, copper has replaced aluminum as an interconnect material in semiconductor devices. However, while copper has superior conductivity to aluminum, a barrier layer must be used with it to stop unwanted diffusion into neighboring materials. To stop this diffusion, the barrier must be made from a material with low copper diffusivity, must coat copper conformally, and must form a completely closed coating. This diffusion barrier should also be as thin as possible so that the advantage gained from copper's increased conductivity is not entirely negated by the wasted volume and added resistivity of the barrier layer. ALD is a coating method that can meet these demands, although sputtered barrier layers remain dominant in the industry.[52]

In Stokhof and coworkers' study, WN_XC_Y was deposited by ALD over two different dielectric layers: SiO_x, deposited by plasma enhanced chemical vapor deposition (PECVD), and Aurora® 2.7, a proprietary low-*k* dielectric. The thickness of the WN_XC_Y layer was controlled by varying the number of ALD cycles. After the first ALD cycle, a strong W LEIS peak appeared at the surface, indicating that the deposition of the WN_XC_Y film had begun. However, a Si surface signal remained clearly visible. This Si surface signal only disappeared after 40 ALD cycles, indicating film closure. The trends were the same for deposition over the Aurora® 2.7 dielectric material, with film closure again occurring after 40 ALD cycles. For this study, the growth rate was 0.8 Å per ALD cycle, meaning that a film thickness of approximately 3.2 nm was needed to achieve a completely closed film. Here, the surface sensitivity of LEIS permitted an analysis that would have been difficult with XPS or ToF-SIMS because these techniques have probe depths that exceed the thicknesses of most of the WC_XN_Y films examined in this study.

While the closure of an ALD-deposited WC_XN_Y film over dielectric layers is a fairly specific example, it again illustrates an important problem—films in semiconductor devices are becoming thinner than the depth of analysis of the dominant surface analysis techniques. For example, gate oxide thicknesses in semiconductors have been in the sub 10 nm range since the early 1990's.[53] When semiconductor technology reached the 22 nm node in 2011, the gate oxide thickness was down to 0.5–0.8 nm.[53] The target for diffusion barrier layer thickness at the 22 nm node is 3 nm.[21] This downward trend in film thicknesses will probably continue as technology advances to the 10 nm and 7 nm nodes. In short, as films get thinner, surface sensitivity will become increasingly important for understanding film properties in semiconductors.

Diffusion is an important process in the fabrication of microfabricated devices. Sometimes it is wanted, as when a wafer is heated to allow dopants to diffuse through a material. Other times, it is destructive, as when copper from interconnects poisons neighboring materials. Because of its extreme surface and near surface sensitivity, LEIS is a powerful tool for understanding diffusion in thin films. Indeed, LEIS' short analysis times make it suitable for time resolved studies. LEIS systems can be outfitted with heating stages to perform *in situ* diffusion studies.

While various useful conclusions can often be drawn about diffusion in a sample simply by observing the changes in the surface signal when a sample is heated, the static depth profile provides more useful and direct information about diffusion in thin films. One reason for this is that surfaces may have different properties than their underlying layers. In 2009, De Rooij-Lohmann *et al.* studied diffusion non-destructively using LEIS static depth profiling.[14] The total depth of their analysis was 5–10 nm. In particular, the authors studied the diffusion of a Mo/Si system (see Fig. 15). These materials find use in extreme UV optics. In order to determine the stopping power of silicon, S_{Si}, the authors prepared Mo films covered with Si films of known thickness (4–7 nm). From this data, they determined that S_{Si} was 36 ± 3 eV nm^{-1}. The samples were then analyzed during heating to 500 °C over a period of 40–50 seconds, and the shape of the Mo depth signal was used to extract the diffusion

Published on 05 April 2016. Downloaded by DTU Library on 4/3/2020 2:12:37 PM.

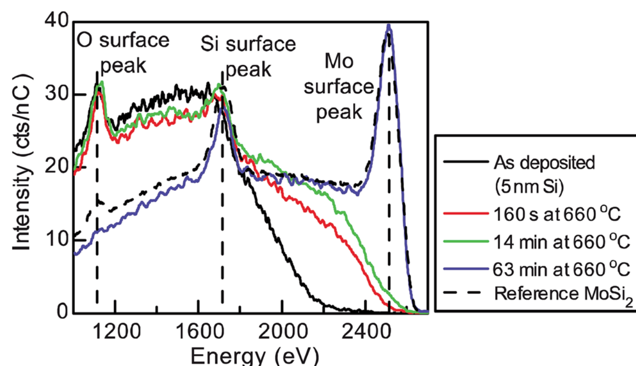

Fig. 15 The evolution of an Mo/Si system at 660 °C as a function of time as probed by LEIS. Reprinted with permission from ["Diffusion and interaction studied nondestructively and in real-time with depth-resolved low energy ion spectroscopy" by V. I. T. A. de Rooij-Lohmann, A. W. Kleyn, F. Bijkerk, H. H. Brongersma, and A. E. Yakshin in *Appl. Phys. Lett.*, **94**, 063107 (2009); DOI: 10.1063/1.3081034]. Copyright [2009], AIP Publishing LLC.

coefficient of Mo in Si for this system. Fig. 16 shows these 500 °C LEIS results. In a follow up study in 2010,[49] they studied the more complex $Mo/B_4C/Si$ system, where B_4C acts a diffusion barrier. Using a methodology similar to the one employed in their previous study, they were able to show two distinct diffusion regimes, which corresponded to amorphous and nanocrystalline $MoSi_2$. The results they obtained by LEIS were supported by transmission electron microscopy (TEM) and hard X-ray XPS (HAXPS) analyses.

The extreme surface sensitivity, straightforward quantitation, static depth profile information, and excellent sputter depth profiling capabilities in LEIS make it a potentially powerful tool for studying semiconductor systems. Its utility for studying the closure of very thin films and understanding diffusion has been noted. We anticipate that because of the recent advances in LEIS instrumentation, there will be more LEIS studies on semiconductor materials.

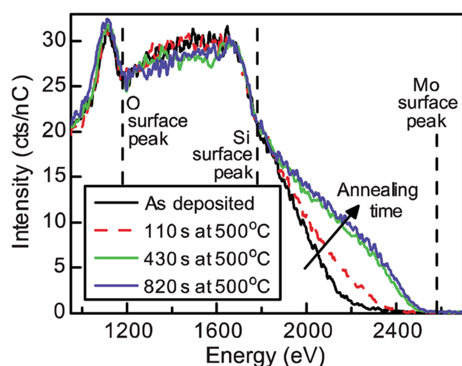

Fig. 16 The evolution of an Mo/Si system at 500 °C as a function of time as probed by LEIS. Reprinted with permission from ["Diffusion and interaction studied nondestructively and in real-time with depth-resolved low energy ion spectroscopy" by V. I. T. A. de Rooij-Lohmann, A. W. Kleyn, F. Bijkerk, H. H. Brongersma, and A. E. Yakshin in *Appl. Phys. Lett.*, **94**, 063107 (2009); DOI: 10.1063/1.3081034]. Copyright [2009], AIP Publishing LLC.

9. LEIS of solid oxide fuel cells[28]

We now discuss some recent publications in which high-sensitivity LEIS has been used to probe the surfaces of materials used in solid oxide fuel cells (SOFCs).

As is the case with all fuel cells, SOFCs directly oxidize a fuel to produce electricity. This is in contrast to the more common combustion-based electrical generation tools that convert fuels to thermal energy, thermal energy to mechanical motion, and then mechanical motion to electricity. As the name implies, SOFCs use solid oxides as electrolytes. Typically, this electrolyte transports oxygen anions from the cathode to the anode. The solid oxide electrolyte is the defining feature in an SOFC, but the cathode and the anode materials must also be able to sustain high temperatures and transport charge carriers.[54] These cathodes and anodes are usually made of ceramics or ceramic–metal hybrids. SOFCs are being researched for their application to clean, efficient energy generation using a variety of fuels. The major obstacle to the widespread adoption of SOFC technology is their high operating temperature.[54] The materials used in SOFCs must function at between 500 and 1000 °C to conduct oxygen anions. These temperature constraints often require that SOFCs undergo a lengthy pre-heating prior to operation, limit the materials that can be used in their construction, and shorten device life spans. This reduces the applicability and increases the cost of this technology.[54] Therefore, much effort has gone into researching materials that can enable SOFCs with lower operating temperatures. The characterization of SOFC materials been an active area for LEIS.[12,13,54–57]

Perovskite type materials are being heavily investigated for SOFC applications. These have the general chemical formula ABX_3, where A is a relatively large cation, B is a relatively small cation, and X is an anion that binds to both. There are other more complex variations of this structure that are also of interest. These are explained in more detail below, as well as in a paper by Druce *et al.*[10] Understanding the surface properties of the materials used as SOFC cathodes is important for improving these devices because oxygen exchange at their surfaces strongly influences device performance – before oxygen ions can be conducted through the electrolyte, O_2 molecules must be split and oxygen incorporated into the material. This is determined by the material's surface properties. With regards to SOFCs, Druce *et al.* noted that "…the exchange of oxygen, at elevated temperatures, between the solid and the ambient gas, mediated by the immediate surface, is a very important process as it determines the oxygen stoichiometry and hence the functional properties".[10] In addition, at elevated temperature, even minor contamination from the bulk of the ceramic can diffuse to the surface, and this can strongly limit its performance. Indeed, only a little bulk contamination is required to form a full monolayer of an alkaline earth oxide, which will significantly compromise the performance of the oxide.[57] Therefore, understanding which cations dominate the surface of the electrolyte is important for understanding oxygen transport through it.

 This journal is © The Royal Society of Chemistry 2016

Published on 05 April 2016. Downloaded by DTU Library on 4/3/2020 2:12:37 PM.

Working towards understanding and improving SOFC cathodes, Burriel *et al.* recently performed a multi-instrument surface analysis of $La_{2-x}Sr_xNiO_{4+\delta}$, which is a promising material for intermediate temperature SOFCs (IT-SOFCs) (they operate from 650 to 800 °C).[13,54] Prior to this analysis, the outer surface of this material had only been studied computationally. The computational results indicated that the material would be terminated in nickel-oxide, where Ni is a B-type cation. Computational models of similar perovskite materials predicted that cathodes would be catalytically inactive if terminated in LaO, where lanthanum is an A-type cation. Burriel's characterization utilized crystal truncation rod (CTR) X-ray scattering, angle resolved XPS (AR-XPS), and LEIS to probe the outer few layers of the material. She notes in her paper that analyzing the outermost layer of a material can be challenging. Any exposure to the atmosphere contaminates a surface with adventitious carbon. Furthermore, as noted above, most surface analysis techniques average over several atomic layers and do not provide information specific to the outermost layer. The LEIS analysis was performed using a Qtac[100] instrument. Two single-crystal samples of different orientation were analyzed, both were cleaved and one was heat treated in air at 450 °C for 72 hours. Prior to analysis, all samples were cleaned with atomic oxygen to remove hydrocarbons. Because each element has its own sensitivity factor, high-purity oxide powders were used as standards to establish sensitivity factors and detection limits for each analyte.

A 5 keV $^{22}Ne^+$ LEIS spectrum from her paper is shown in Fig. 17. Contrary to the predictions of the computational model, the LEIS spectrum shows signals for the A-type cations, Sr and La, while no Ni is detected at the surface. Both of the samples produced similar results. While neither CTR X-ray scattering nor AR-XPS gave a quantitative analysis of the composition of the outermost layer, both provided information about the near-surface region. CTR-X-ray scattering is a modeling based technique (analogous in some sense to ellipsometry) – data are obtained and fit with either theoretical or empirical models, and conclusions about the material are drawn based on which model gives the best fit. In this case, a model of a La/Sr oxide terminated material provided a good match to the experimental data with some deviations attributed to surface effects, while a model of an NiO_2 terminated material gave a poor fit. This is in good agreement with the LEIS results. Using AR-XPS, the ratio of lanthanum and strontium to nickel ((La + Sr)/Ni) ratio was calculated at depths ranging from 0.6 to 7.0 nm. The data were compared to a theoretical ratio based on the stoichiometry of the bulk material, which was calculated to be 2.0. At a depth of analysis of 7.0 nm, the measured ratio was at 2.3, close to the bulk value, while the ratios at depths of 1.8 and 0.6 nm were 8.5 and 5.3, respectively. These results indicate that the near-surface region is enriched in La and Sr, again supporting the La/Sr oxide terminated surface suggested by LEIS. When three established surface analysis techniques support the same conclusion, it is probably true, and of course, it is almost always better to probe a material with multiple analytical techniques than a single one.[26,58,59]

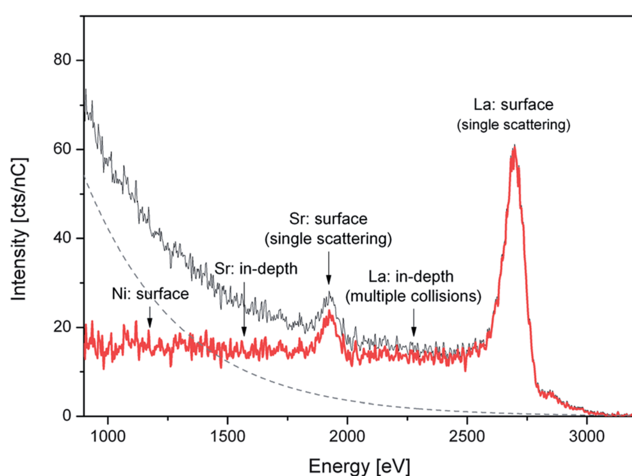

Fig. 17 LEIS spectrum of $La_{1.67}Sr_{0.33}NiO_{4+\delta}$ shown with and without a background correction. Reproduced from 'Absence of Ni on the outer surface of Sr doped La_2NiO_4 single crystals' by Mónica Burriel, Stuart Wilkins, John P. Hill, Miguel A. Muñoz-Márquez, Hidde H. Brongersma, John A. Kilner, Mary P. Ryan, and Stephen J. Skinner in *Energy Environ. Sci.*, 2014, 7, 311–316, DOI: 10.1039/c3ee41622d with permission of The Royal Society of Chemistry.[13]

These results challenged the previous computational models of oxygen transport through this cathode material. With regards to the role LEIS analysis played in this study, the author wrote, "…it is clear that the unique monolayer sensitivity provided by LEIS, complemented by other state-of-the-art surface techniques, can provide a complete picture of the surface and near-surface chemistry of this important class of materials", and that "…the new surface information provided by these techniques will significantly contribute to the understanding of surface processes in mixed conducting materials…".[13]

In another study, Druce *et al.* used LEIS in conjunction with a sputter beam to depth profile three polycrystalline perovskite-based electroceramics for use in SOFC applications: $La_{0.6}Sr_{0.4}Co_{0.2}Fe_{0.8}O_{0.3-\delta}$ (LSCF-113), $GdBaCo_2O_{5+\delta}$ (GBCO-1125), and $La_2NiO_{4+\delta}$ (LNO-214).[10] LCSF-113 has the single perovskite structure, ABO_3, GBCO-1125 has the ordered double perovskite structure, $AA'B_2O_{5+\delta}$, where A and A′ cations alternate in layers of the structure, and LNO-214 has the Ruddelson–Popper structure, with a formula of $A_2BO_{4+\delta}$, where layers of the perovskite structure are interrupted by layers of AO with the rock salt structure. For this study, the samples were pretreated at high temperature in oxygen to mimic their operating conditions. As in the example above, the samples were cleaned with atomic oxygen prior to LEIS analysis to remove hydrocarbon contaminants. Three spectra at different sputtering depths are shown for each sample in Fig. 18. Interestingly, spectra taken at different depths show different compositions. The dominant species at the surfaces of these materials are Sr, Ba, and La, for LSCF-113, GBCO-1125, and LNO-214, respectively. This means that for LCSF-113, the A-site cation terminates the surface. For GBCO-1125, which consists of alternating layers of two oxides, the A′ site cation terminates the material, and for LNO-214, the A-site cation terminates the material. At its outer surface, LNO-214 additionally shows a Pb peak that is attributed to

Published on 05 April 2016. Downloaded by DTU Library on 4/3/2020 2:12:37 PM.

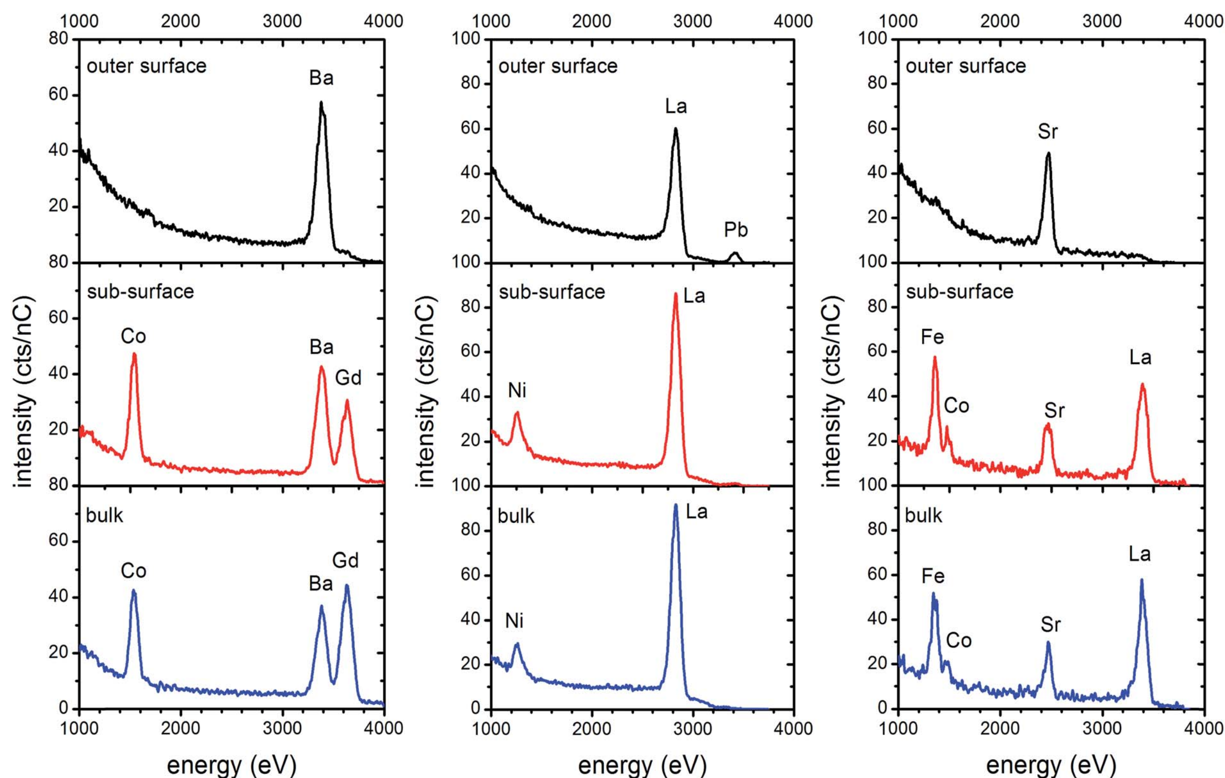

Fig. 18 LEIS spectra of three SOFC materials: (a) GBCO-1125 (left), (b) LNO 214 (middle), and (c) LSCF-113 (right). Spectra taken at the outer surface (top), the near surface region (middle), and the bulk of the material (bottom). Data were originally plotted in a different format in 'Surface termination and subsurface restructuring of perovskite-based solid oxide electrode materials' by J. Druce, H. T'ellez, M. Burriel, M. D. Sharp, L. J. Fawcett, S. N. Cook, D. S. McPhail, T. Ishihara, H. H. Brongersma, and J. A. Kilner in *Energy & Environmental Science*, 2014, DOI: 10.1039/c4ee01497a.

contamination in the starting materials used for the synthesis. Here, Pb is only detectable at the outermost surface, indicating that it preferentially segregates to the surface. With sputtering of this material, no Pb is observed and LEIS analysis gives concentrations corresponding to the theoretical bulk stoichiometry. Given that the properties of these electrode materials depend so much on their surface compositions, these experiments provide valuable information. They clearly demonstrate that the surfaces of these materials can vary significantly from their bulk compositions. The authors emphasize that while other surface analytical techniques have shown enrichment of certain species near the surface of these materials, LEIS, with its extreme surface sensitivity, was unique in its ability to provide information about the composition of the outermost layer.

While we have only shown two examples here related to the development of better materials for SOFC applications, it is easy to see how information obtained by LEIS would be generally useful for understanding a variety of materials, *e.g.*, gas sensors, catalysts, *etc.*

In summary, LEIS has revealed how several materials proposed for SOFC applications are terminated. In one case the results were contrary to the predictions of computational models. Both papers highlighted herein noted that while other more conventional surface analytical techniques provide valuable information about the near-surface region of materials, only LEIS provides a quantitative elemental analysis of the outermost atomic layer. This definitive information about surface composition is obviously of value for the characterization and development of SOFCs, where surface composition plays an important role in catalysis and oxygen anion transport.

10. LEIS of catalysts[60]

The basic purpose of a catalyst is to speed up a chemical reaction by lowering its activation energy. Industrially, heterogeneous catalysts, catalysts that differ in phase from their reactants and products, are preferred because they are easily separable from chemical reagents. That is, they are more easily recovered and will not contaminate the product. In practice, this means that most industrial catalysts are solids.[61] Catalysts have changed our world. For example, the level of agricultural production needed to sustain the world's population would not be possible without the Haber–Bosch process for ammonia production, which depends on a heterogeneous catalyst.[61] Most industrially important building block molecules, such as ammonia, benzene, sulfuric acid, and styrene are synthesized with the help of heterogeneous catalysts.[62] Petroleum refinement also depends heavily on the use of heterogeneous catalysts.[62] Because catalysts are so pervasive, there is an ongoing need to characterize them, both to understand their fundamental science and also to better synthesize them.

 This journal is © The Royal Society of Chemistry 2016

Published on 05 April 2016. Downloaded by DTU Library on 4/3/2020 2:12:37 PM.

Catalysis depends on reactants interacting with the catalyst in a way that favors the desired chemical reaction. In the case of solid catalysts this means that catalysis generally happens at the outermost atomic layer of the material. Accordingly, LEIS, with its extreme surface sensitivity, is especially well suited for analyzing these materials. And many heterogeneous catalysts are complex, multicomponent systems. For example, the catalyst used in the Haber–Bosch process consists of magnetite (Fe_3O_4) with 2.5–4% Al_2O_3, 0.5–1.2% K_2O, 2.0–3.5% CaO and 0.0–1.0% MgO.[61] In such materials, the surface concentration of a species can vary significantly from its bulk concentration. LEIS provides useful information in these situations by directly measuring the surface concentrations of all species. Additionally LEIS static and sputter depth profiles can be used to determine how the surface composition varies from the bulk stoichiometry. Ter Veen *et al.* published a short article on the application of LEIS to a catalyst.[37] They stated that: "…the availability of a technique that analyzes the chemical composition of this [outermost] layer is of crucial importance in the fundamental study of catalysis as well as in the optimization of industrial catalysts." In contrast, XPS, with its greater depth of analysis provides less information about the outermost atomic layer where catalysis takes place. An article by Celaya Sanfiz *et al.*[63] states that: "…in cases where conventional surface analytic techniques, such as XPS, do not show correlation with the catalytic activity, the extreme surface sensitivity of LEIS gives a direct relationship between composition and catalysis." To add to the utility of LEIS, LEIS instruments are often equipped with environmental chambers wherein the working environment of a catalyst can be simulated by heating it to a desired temperature and dosing it with gases. Here, a reaction can be rapidly quenched before the sample is transferred to the analytical chamber. This allows a surface to be studied at or near its operating state, giving insight into the surface composition of the catalyst as it is used. LEIS is relatively insensitive to surface roughness so real industrial catalysts, not just model, planar systems, can be analyzed.

Below, we discuss two examples of LEIS studies of heterogeneous catalysts.

Celaya Sanfiz *et al.* performed a detailed analysis of an $MoVTeNbO_x$ catalyst, which is used for the selective oxidation of light alkanes, *e.g.*, propane to acrylic acid.[63] Previously, this catalyst had shown enhanced activity after grinding. The authors were interested in studying the (001) plane of the M1 phase of the catalyst. It had previously been suggested that this plane had active and selective sites for partial oxidation reactions. When fractured (ground), M1 phase crystals expose their (001) plane. Accordingly, the authors coated catalyst crystals with silica and then ground them. In theory, the silica should have covered all the planes except for those that were exposed by fracturing during grinding, which, again, would preferentially expose (001) crystal planes. They used uncoated crystallites as a control, and analyzed the catalytic activity of the silica-coated and ground, and untreated crystals. LEIS played an important role in their analysis. First, it was used to determine whether the silica-coated samples had been completely coated. The absence of any surface signals except for Si and O showed that the coating was complete. Based on depth profile information from LEIS, the thickness of this coating was estimated to range from a few atomic layers up to about 20 nm. TEM supported this conclusion. LEIS was also used to determine how much catalyst surface was exposed during grinding. As expected, the percentages of V_2O_5, Nb_2O_5, MoO_3, and TeO_3 were much lower in the coated, ground samples than in the untreated samples. By comparing the signal ratios between the samples, the authors determined that 70% of the ground samples remained coated in silica, while 30% of the surface was freshly exposed. Here, LEIS yielded a much higher percentage of newly exposed surface area than did a shape analysis using SEM images, indicating that in addition to fracturing, some silica was abraded from the particles during the grinding process. This hypothesis was supported by TEM images taken post-grinding. To determine if the (001) plane played a special role in determining the selectivity of the catalyst, the authors compared the catalytic activity of the coated, ground sample to the uncoated one. When normalized for exposed catalyst area, the catalytic activity was about the same for both samples. Based on the results, the authors concluded that the selectivity and activity of this catalyst could not be due uniquely to the (001) plane of the material.

LEIS was also used to probe the composition of this catalyst. Given the complexity of this material, a calibration plot could not be used for quantitation, and instead, oxide powders (SiO_2, V_2O_5, Nb_2O_5, MoO_3, TeO_2) were used as references. The authors noted that, because these samples were cleaned with atomic oxygen before analysis, they expected all surface species to be in their highest oxidation states, making oxide powders the correct choice for standards. Energy dispersive X-ray analysis (EDX) was used to measure the bulk composition, and the bulk and surface compositions were compared. For the unground material, the surface was enriched in tellurium and deficient in vanadium. For the coated, ground material, the surface was enriched in tellurium and deficient in molybdenum.

Phivilay *et al.*[64] recently used LEIS in the multi-instrument characterization of a $(Rh_{2-y}Cr_yO_3)$/GaN catalyst, which is used in the UV splitting of water for production of H_2 and O_2. Their goal was to understand the relationship between catalyst structure and photoactivity. While GaN is catalytically inactive in splitting water, the addition of $Rh_{2-y}Cr_yO_3$ nanoparticles to its surface makes it active. Their catalyst system is depicted in Fig. 19. In addition to probing the surface with LEIS, the authors used high-resolution XPS, Raman spectroscopy, ultraviolet/visible spectroscopy (UV-Vis), and photoluminescence to understand their material. This study is an excellent example of how bulk techniques (Raman, UV-Vis), and in particular the multi-instrument characterization of materials,[26,40,58] play a role in understanding surfaces. Their UV-Vis analysis showed that the addition of $(Rh_{2-y}Cr_yO_3)$ nanoparticles to the GaN surface resulted in no change in the bandgap of the bulk GaN, implying that the changes they observed must be occurring at the material's surface. HR-XPS provided information about the chemical states of the species in the system. Based on chemical shifts, the Rh and Cr in the outer 3 nanometers of this material were assigned to their +3 oxidation states. There was no Cr^{6+} or

Published on 05 April 2016. Downloaded by DTU Library on 4/3/2020 2:12:37 PM.

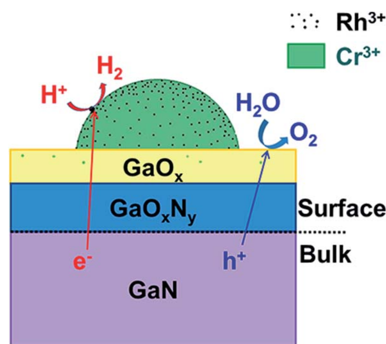

Fig. 19 Representation of a $(Rh_{2-y}Cr_yO_3)$/GaN catalyst. Reprinted (adapted) with permission from ('Fundamental Bulk/Surface Structure–Photoactivity Relationships of Supported $(Rh_{2-y}Cr_yO_3)$/GaN Photocatalysts' by Somphonh P. Phivilay, Charles A. Roberts, Alexander A. Puretzky, Kazunari Domen, and Israel E. Wachs, DOI: 10.1021/jz401884c, *J. Phys. Chem. Lett.*, 2013, **4**, 3719–3724). Copyright (2013) American Chemical Society.

metallic Rh at the surface. LEIS played an important role in this work by providing compositional information for GaN and for the $(Rh_{2-y}Cr_yO_3)$/GaN catalyst. In addition to analyzing the surface region, the near surface region was probed by depth profiling. Interestingly, for the GaN, there was virtually no N signal at the surface. With sputtering, the N signal gradually appeared and the oxygen signal gradually decreased. This indicates that the stoichiometry of the outermost layer is best described as GaO_x, and the subsurface region is best described as GaO_xN_y. The authors noted that this was the first time a surface characterization had revealed this compositional information. The Ne^+ LEIS spectrum for $(Rh_{2-y}Cr_yO_3)$/GaN showed contamination from tin and barium. Again, contaminants often diffuse to the surface of a material and become

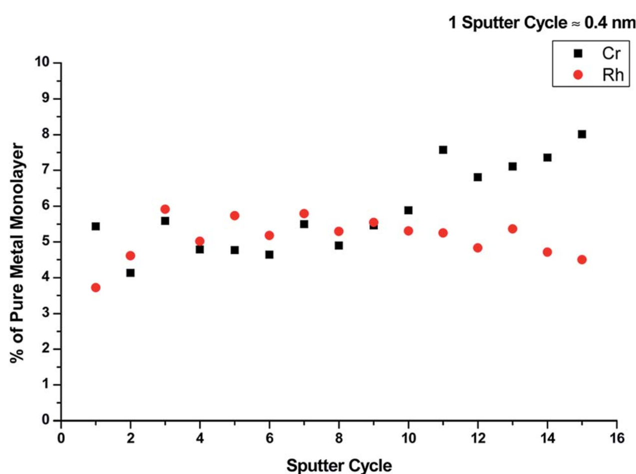

Fig. 20 Depth profile concentrations of Cr and Rh in a $(Rh_{2-y}Cr_yO_3)$/GaN catalyst as determined by LEIS. Reprinted (adapted) with permission from ('Fundamental Bulk/Surface Structure–Photoactivity Relationships of Supported $(Rh_{2-y}Cr_yO_3)$/GaN Photocatalysts' by Somphonh P. Phivilay, Charles A. Roberts, Alexander A. Puretzky, Kazunari Domen, and Israel E. Wachs, DOI: 10.1021/jz401884c, *J. Phys. Chem. Lett.*, 2013, **4**, 3719–3724). Copyright (2013) American Chemical Society.

concentrated there to minimize surface free energy. The authors attributed the contamination they found to the $(Rh_{2-y}Cr_yO_3)$ precursors. A depth profile (Fig. 20) showed that the material became richer in Cr with increasing sputter depth. LEIS measurements indicated that both species were enriched in the near surface region compared to their expected bulk concentrations. The authors used pure metal references to quantify the surface coverage of Cr and Rh because they were interested in the surface coverages of the pure metals rather than their oxides. Using the quantitative information they obtained about the Rh concentration at the surface, they calculated a turnover frequency (TOF) for the material, which is defined as the number of H_2 molecules produced per exposed Rh^{3+} site per second. Obviously, this calculation would not have been possible without a technique capable of quantifying the Rh concentration at the final surface. LEIS proved to be very useful in this study. The authors were surprised by the composition of the outer layers of their GaN film, and by the fact that the surface was significantly enriched in Rh and Cr. They were also surprised by the presence of Sn and Ba. Quantitative information about Rh was used to calculate the turnover frequency for hydrogen.

11. Conclusion

LEIS is a powerful analytical tool for understanding the outermost atomic layer of a material. The operating principles of LEIS, summarized in eqn (1), can be understood in terms of classical physics. Surface signals in LEIS are Gaussian, while the signal in LEIS static depth profiles appears as a tail on the lower energy side of the surface signal. The components of a typical LEIS system are an ion source, a kinetic energy analyzer, and a detector. All of these are housed in a high vacuum chamber. Advances in detector geometry have significantly improved the sensitivity of the technique. Quantitation in LEIS is generally straightforward, and with very few exceptions, there is no matrix effect in LEIS. For some systems, LEIS can be accomplished without the use of reference samples. For more complex systems, reference powders are used to establish sensitivity factors for each element.

The applications we have shown demonstrate the unique information LEIS can provide. In a study of ALD deposited gate-oxide films, the extreme surface sensitivity of LEIS was valuable for understanding film closure. The static depth profiling capabilities of LEIS are useful in characterizing the diffusion in thin films for extreme UV optics. In the study of solid-oxide fuel cells, LEIS provided information about the outermost surface that challenged previous conclusions from computational studies about the structure of the material. LEIS is extremely useful for studying catalysts, where the outermost layer plays a determining role in the activity and rate of catalysis.

We again emphasize the importance of multi-instrument surface and material characterization.[26,58] The fact that LEIS is insensitive to the chemical environments of analytes makes it powerful for quantifying surface compositions. LEIS is complementary to XPS and ToF-SIMS. In general, it is much more surface sensitive than either of these two techniques.

 This journal is © The Royal Society of Chemistry 2016

Published on 05 April 2016. Downloaded by DTU Library on 4/3/2020 2:12:37 PM.

However, it only provides information about elemental composition, whereas ToF-SIMS gives molecular information, and XPS is sensitive to chemical environment. We believe that in the future more studies involving all three techniques will be performed, and that this approach will become increasingly necessary for the full characterization of advanced materials.

Acknowledgements

We acknowledge Vacuum Technology & Coating (VT&C) magazine for giving us full permission to use text and figures in this document that previously appeared in a series of installments written for VT&C.[7,28,32,33,39,60,65] In general, this material is not marked by quotation marks or otherwise specifically identified.

References

1 D. P. Smith, Scattering of Low-Energy Noble Gas Ions from Metal Surfaces, *J. Appl. Phys.*, 1967, **38**(1), 340–347.
2 H. H. Brongersma and P. M. Mu, Analysis of the outermost atomic layer of a surface by low-energy ion scattering, *Surf. Sci.*, 1973, **35**, 393–412.
3 R. P. N. Bronckers and A. G. J. d. Wit, Reconstruction of the oxygen-covered Cu{110} surface identified with low energy Ne^+ and H_2O^+ ion scattering, *Surf. Sci.*, 1981, **112**(1–2), 133–152.
4 H. Engelhardt, W. Bäck, D. Menzel and H. Liebl, Novel charged particle analyzer for momentum determination in the multichanneling mode: I. Design aspects and electron/ion optical properties, *Rev. Sci. Instrum.*, 1981, **52**(6), 835–839.
5 H. Engelhardt, A. Zartner and D. Menzel, Novel charged particle analyzer for momentum determination in the multichanneling mode. II. Physical realization, performance tests, and sample spectra, *Rev. Sci. Instrum.*, 1981, **52**(8), 1161–1173.
6 H. H. Brongersma, M. Draxler, M. de Ridder and P. Bauer, Surface composition analysis by low-energy ion scattering, *Surf. Sci. Rep.*, 2007, **62**(3), 63–109.
7 C. V. Cushman, M. R. Linford and T. Grehl, Low Energy Ion Scattering (LEIS). I. The Fundamentals, *Vacuum Technology & Coating*, April, 2015, pp. 26–33.
8 H. H. Brongersma, T. Grehl, P. A. van Hal, N. C. W. Kuijpers, S. G. J. Mathijssen, E. R. Schofield, R. A. P. Smith and H. R. J. ter Veen, High-sensitivity and high-resolution low-energy ion scattering, *Vacuum*, 2010, **84**(8), 1005–1007.
9 H. H. Brongersma, M. de Ridder, A. Gildenpfennig and M. M. Viitanen, Insight in the outside: materials science at the atomic level using LEIS, *J. Eur. Ceram. Soc.*, 2003, **23**(15), 2761–2767.
10 J. Druce, H. Téllez, M. Burriel, M. D. Sharp, L. J. Fawcett, S. N. Cook, D. S. McPhail, T. Ishihara, H. H. Brongersma and J. A. Kilner, Surface termination and subsurface restructuring of perovskite-based solid oxide electrode materials, *Energy Environ. Sci.*, 2014, **7**(11), 3593–3599.
11 V. R. Stamenkovic, B. Fowler, B. S. Mun, G. Wang, P. N. Ross, C. A. Lucas and N. M. Marković, Improved Oxygen Reduction Activity on $Pt_3Ni(111)$ via Increased Surface Site Availability, *Science*, 2007, **315**(5811), 493–497.
12 H. Téllez, A. Aguadero, J. Druce, M. Burriel, S. Fearn, T. Ishihara, D. S. McPhail and J. A. Kilner, New perspectives in the surface analysis of energy materials by combined time-of-flight secondary ion mass spectrometry (ToF-SIMS) and high sensitivity low-energy ion scattering (HS-LEIS), *J. Anal. At. Spectrom.*, 2014, **29**(8), 1361.
13 M. Burriel, S. Wilkins, J. P. Hill, M. A. Muñoz-Márquez, H. H. Brongersma, J. A. Kilner, M. P. Ryan and S. J. Skinner, Absence of Ni on the outer surface of Sr doped La_2NiO_4 single crystals, *Energy Environ. Sci.*, 2014, **7**(1), 311–316.
14 V. I. T. A. de Rooij-Lohmann, A. W. Kleyn, F. Bijkerk, H. H. Brongersma and A. E. Yakshin, Diffusion and interaction studied nondestructively and in real-time with depth-resolved low energy ion spectroscopy, *Appl. Phys. Lett.*, 2009, **94**(6), 063107.
15 S. Rubin, Surface Analysis by Charged Particle Spectroscopy, *Nucl. Instrum. Methods*, 1959, **5**, 177–183.
16 H. H. Brongersma, A. Gildenpfennig, A. W. D. v. d. Gon, R. D. v. d. Grampel, W. P. A. Jansen, A. Knoester, J. Laven and M. M. Viitanen, Insight in the outside: New applications of low-energy ion scattering, *Nucl. Instrum. Methods Phys. Res., Sect. B*, 2002, **190**(1–4), 11–18.
17 J. P. Biersack and L. G. Haggmark, A Monte Carlo computer program for the transport of energetic ions in amorphous targets, *Nucl. Instrum. Methods*, 1980, **174**(1–2), 257–269.
18 J. F. Ziegler, J. P. Biersack and M. D. Ziegler, *SRIM: the stopping and range of ions in matter*, SRIM Co., Chester, Md, 2012.
19 J. F. Ziegler, M. D. Ziegler and J. P. Biersack, SRIM – The stopping and range of ions in matter, *Nucl. Instrum. Methods Phys. Res., Sect. B*, 2010, **268**(11–12), 1818–1823.
20 P. Brüner, T. Grehl, H. Brongersma, B. Detlefs, E. Nolot, H. Grampeix, E. Steinbauer and P. Bauer, Thin film analysis by low-energy ion scattering by use of TRBS simulations, *J. Vac. Sci. Technol., A*, 2015, **33**(1), 01A122.
21 J. Gambino, 8-Process Technology for Copper Interconnects, in *Handbook of Thin Film Deposition* ed. K. Seshan, William Andrew Publishing, Oxford, 3rd edn, 2012; pp. 221–269.
22 G. Ye, H. Wang, S. Arulkumaran, G. I. Ng, R. Hofstetter, Y. Li, M. Anand, K. Ang, Y. Maung and S. C. Foo, Atomic layer deposition of ZrO_2 as gate dielectrics for AlGaN/GaN metal-insulator-semiconductor high electron mobility transistors on silicon, *Appl. Phys. Lett.*, 2013, **103**(14), 142109.
23 H. Liu and P. D. Ye, Dual-Gate MOSFET with Atomic-Layer-Deposited as Top-Gate Dielectric, *IEEE Electron Device Lett.*, 2012, **33**(4), 546–548.
24 R. Suzuki, N. Taoka, M. Yokoyama, S. Lee, S. Kim, T. Hoshii, T. Yasuda, W. Jevasuwan, T. Maeda and O. Ichikawa, 1 nm-capacitance-equivalent-thickness HfO_2/Al_2O_3/InGaAs metal-oxide-semiconductor structure with low interface trap density and low gate leakage current density, *Appl. Phys. Lett.*, 2012, **100**(13), 132906.
25 H. Wang, N. Madaan, J. Bagley, A. Diwan, Y. Liu, R. C. Davis, B. M. Lunt, S. J. Smith and M. R. Linford, Spectroscopic

View Article Online

Published on 05 April 2016. Downloaded by DTU Library on 4/3/2020 2:12:37 PM.

ellipsometric modeling of a Bi–Te–Se write layer of an optical data storage device as guided by atomic force microscopy, scanning electron microscopy, and X-ray diffraction, *Thin Solid Films*, 2014, **569**, 124–130.

26 D. S. Jensen, S. S. Kanyal, N. Madaan, J. M. Hancock, A. E. Dadson, M. A. Vail, R. Vanfleet, V. Shutthanandan, Z. Zhu, M. H. Engelhard and M. R. Linford, Multi-instrument characterization of the surfaces and materials in microfabricated, carbon nanotube-templated thin layer chromatography plates. An analogy to 'The Blind Men and the Elephant', *Surf. Interface Anal.*, 2013, **45**(8), 1273–1282.

27 B. Singh, S. J. Smith, D. S. Jensen, H. F. Jones, A. E. Dadson, P. B. Farnsworth, R. Vanfleet, J. K. Farrer and M. R. Linford, Multi-instrument characterization of five nanodiamond samples: a thorough example of nanomaterial characterization, *Anal. Bioanal. Chem.*, 2015, 1–18.

28 C. V. Cushman, T. Grehl and M. R. Linford, Low Energy Ion Scattering (LEIS). II. Instrumentation and Application to Solid Oxide Fuel Cells, *Vacuum Technology & Coating*, May, 2015, pp. 28–34.

29 P. A. J. Ackermans, P. F. H. M. Van Der Meulen, H. Ottevanger, F. E. Van Straten and H. H. Brongersma, Simultaneous energy and angle resolved ion scattering spectroscopy, *Nucl. Instrum. Methods Phys. Res., Sect. B*, 1988, **35**(3–4), 541–543.

30 H. H. Brongersma, T. Grehl, E. R. Schofield, R. A. P. Smith and H. R. J. ter Veen, Analysis of the Outer Surface of Platinum-Gold Catalysts by Low-Energy Ion Scattering, *Platinum Met. Rev.*, 2010, **54**(2), 81–87.

31 S. Caporali, U. Bardi and A. Lavacchi, X-ray photoelectron spectroscopy and low energy ion scattering studies on 1-butyl-3-methyl-imidazolium bis(trifluoromethane) sulfonimide, *J. Electron Spectrosc. Relat. Phenom.*, 2006, **151**(1), 4–8.

32 C. V. Cushman, P. Brüner, J. Zakel, G. Major, B. M. Lunt, T. Grehl, N. J. Smith and M. R. Linford, A Pictorial View of LEIS and ToF-SIMS Instrumentation, *Vacuum Technology & Coating*, February, 2016, pp. 27–35.

33 C. V. Cushman, M. R. Linford and T. Grehl, Low Energy Ion Scattering (LEIS). III. Quantitation in LEIS, *Vacuum Technology & Coating*, June, 2015, pp. 32–35.

34 L. Adriaensen, F. Vangaever and R. Gijbels, Metal-Assisted Secondary Ion Mass Spectrometry: Influences of Ag and Au Deposition on Molecular Ion Yields, *Anal. Chem.*, 2004, **76**, 6777–6785.

35 A. Delcorte and P. Bertrand, Interest of silver and gold metallization for molecular SIMS and SIMS imaging, *Appl. Surf. Sci.*, 2004, **231–232**, 250–255.

36 A. Delcorte, N. Médard and P. Bertrand, Organic Secondary Ion Mass Spectrometry: Sensitivity Enhancement by Gold Deposition, *Anal. Chem.*, 2002, **74**(19), 4955–4968.

37 H. R. J. ter Veen, T. Kim, I. E. Wachs and H. H. Brongersma, Applications of High Sensitivity-Low Energy Ion Scattering (HS-LEIS) in heterogeneous catalysis, *Catal. Today*, 2009, **140**(3–4), 197–201.

38 S. Průša, P. Procházka, P. Bábor, T. Šikola, R. ter Veen, M. Fartmann, T. Grehl, P. Brüner, D. Roth, P. Bauer and H. H. Brongersma, Highly Sensitive Detection of Surface and Intercalated Impurities in Graphene by LEIS, *Langmuir*, 2015, **31**(35), 9628–9635.

39 C. V. Cushman, T. Grehl and M. R. Linford, Low Energy Ion Scattering (LEIS). V. Static and Sputter Depth Profiling and Application to Semiconductor Devices, *Vacuum Technology & Coating*, November, 2015, pp. 28–33.

40 M. R. Linford, Introduction to Surface and Material Analysis and to Various Analytical Techniques, *Vacuum Technology & Coating*, April, 2014, pp. 27–32.

41 M. R. Linford, The Gaussian–Lorentzian Sum, Product, and Convolution (Voigt) Functions Used in Peak Fitting XPS Narrow Scans, and an Introduction to the Impulse Function, *Vacuum Technology & Coating*, July, 2014, pp. 27–34.

42 M. R. Linford, An Introduction to Time-of-Flight Secondary Ion Mass Spectrometry (ToF-SIMS), *Vacuum Technology & Coating*, April, 2014, pp. 30–35.

43 B. Singh, D. Velázquez, J. Terry and M. R. Linford, Comparison of the equivalent width, the autocorrelation width, and the variance as figures of merit for XPS narrow scans, *J. Electron Spectrosc. Relat. Phenom.*, 2014, **197**, 112–117.

44 B. Singh, D. Velázquez, J. Terry and M. R. Linford, The equivalent width as a figure of merit for XPS narrow scans, *J. Electron Spectrosc. Relat. Phenom.*, 2014, **197**, 56–63.

45 L. Yang, Y.-Y. Lua, G. Jiang, B. J. Tyler and M. R. Linford, Multivariate analysis of TOF-SIMS spectra of monolayers on scribed silicon, *Anal. Chem.*, 2005, **77**(14), 4654–4661.

46 L. Yang, N. Shirahata, G. Saini, F. Zhang, L. Pei, M. C. Asplund, D. G. Kurth, K. Ariga, K. Sautter and T. Nakanishi, Effect of surface free energy on PDMS transfer in microcontact printing and its application to ToF-SIMS to probe surface energies, *Langmuir*, 2009, **25**(10), 5674–5683.

47 V. Gupta, H. Ganegoda, M. H. Engelhard, J. Terry and M. R. Linford, Assigning Oxidation States to Organic Compounds *via* Predictions from X-ray Photoelectron Spectroscopy: A Discussion of Approaches and Recommended Improvements, *J. Chem. Educ.*, 2014, **91**(2), 232–238.

48 S. Hofmann, *Auger- and X-ray Photoelectron Spectroscopy in Materials Science,* Springer, Berlin, 2013, pp. 297–408.

49 V. I. T. A. de Rooij-Lohmann, A. E. Yakshin, R. W. E. van de Kruijs, E. Zoethout, A. W. Kleyn, E. G. Keim, M. Gorgoi, F. Schäfers, H. H. Brongersma and F. Bijkerk, Enhanced diffusion upon amorphous-to-nanocrystalline phase transition in Mo/B_4C/Si layered systems, *J. Appl. Phys.*, 2010, **108**(1), 014314.

50 R. ter Veen, M. Fartmann, R. Kersting and B. Hagenhoff, Combining dynamic and static depth profiling in low energy ion scattering, *J. Vac. Sci. Technol., A*, 2013, **31**(1), 01A113.

51 M. Stockhof, H. Sprey, W.-M. Li, M. d. Ridder, H. Sprey, S. Haukka and H. Brongersma, LEIS Study of ALD WN_XC_Y Growth on Dielectric Layers, *ECS Trans.*, 2006, **1**(10), 71–77.

 This journal is © The Royal Society of Chemistry 2016

Published on 05 April 2016. Downloaded by DTU Library on 4/3/2020 2:12:37 PM.

52 V. Jousseaume, P.-H. Haumesser, C. Pernel, J. Butterbaugh, S. Maîtrejean and D. Louis, Chemistry in Interconnects, in *Chemistry in Microelectronics*, John Wiley & Sons, Inc., 2013, pp. 81–186.
53 K. Seshan, 2-Scaling and Its Implications for the Integration and Design of Thin Film and Processes, in *Handbook of Thin Film Deposition*, ed. K. Seshan, William Andrew Publishing, Oxford, 3rd edn, 2012; pp. 19–40.
54 E. D. Wachsman and K. T. Lee, Lowering the Temperature of Solid Oxide Fuel Cells, *Science*, 2011, **334**(6058), 935–939.
55 J. Druce, H. Téllez, N. Simrick, T. Ishihara and J. Kilner, Surface composition of solid oxide electrode structures by laterally resolved low energy ion scattering (LEIS), *Int. J. Hydrogen Energy*, 2014, **39**(35), 20850–20855.
56 J. Druce, T. Ishihara and J. Kilner, Surface composition of perovskite-type materials studied by Low Energy Ion Scattering (LEIS), *Solid State Ionics*, 2014, **262**, 893–896.
57 M. de Ridder, R. G. van Welzenis, H. H. Brongersma, S. Wulff, W. F. Chu and W. Weppner, Discovery of the rate limiting step in solid oxide fuel cells by LEIS, *Nucl. Instrum. Methods Phys. Res., Sect. B*, 2002, **190**(1–4), 732–735.
58 G. Jiang, F. Rivera, S. S. Kanyal, R. C. Davis, R. Vanfleet, B. M. Lunt, V. Shutthanandan and M. R. Linford, Characterization of the plastic substrates, the reflective layers, the adhesives, and the grooves of today's archival-grade recordable DVDs, *Opt. Eng.*, 2011, **50**(1), 015201.
59 M. R. Linford, The Blind Men and the Elephant as a Metaphor for the Multi-Instrument Analysis of Surfaces and Materials. Analysis of the Surfaces and Materials in Microfabricated Thin Layer Chromatography Plates, *Vacuum Technology & Coating*, 2014.
60 C. V. Cushman, T. Grehl and M. R. Linford, Low Energy Ion Scattering (LEIS). IV. Applications to Catalysis, *Vacuum Technology & Coating*, September, 2015, pp. 34–37.
61 J. R. H. Ross, Chapter 1-Heterogeneous Catalysis – Chemistry in Two Dimensions, in *Heterogeneous Catalysis*, ed. J. R. H. Ross, Elsevier, Amsterdam, 2012, pp. 1–15.
62 K. W. Kolasinski, Heterogeneous Catalysis, in *Surface Science*, John Wiley & Sons, Ltd, 2012, pp. 267–303.
63 A. Celaya Sanfiz, T. W. Hansen, A. Sakthivel, A. Trunschke, R. Schlögl, A. Knoester, H. H. Brongersma, M. H. Looi and S. B. A. Hamid, How important is the (001) plane of M1 for selective oxidation of propane to acrylic acid?, *J. Catal.*, 2008, **258**(1), 35–43.
64 S. P. Phivilay, C. A. Roberts, A. A. Puretzky, K. Domen and I. E. Wachs, Fundamental Bulk/Surface Structure–Photoactivity Relationships of Supported $(Rh_{2-y}Cr_yO_3)$/GaN Photocatalysts, *J. Phys. Chem. Lett.*, 2013, **4**(21), 3719–3724.
65 M. R. Linford, A Discussion of Aspects of a Paper by Caporali, Bardi, and Lavacchi on LEIS and XPS, *Vacuum Technology & Coating*, May, 2014.